Atmos. Meas. Tech. Discuss., doi:10.5194/amt-2015-340, 2016
Manuscript under review for journal Atmos. Meas. Tech.
Published: 18 January 2016

Atmospheric Measurement Techniques Discussions

Polarimetric remote sensing in O_2 A and B bands: Sensitivity study and information content analysis for vertical profile of aerosols

Shouguo Ding, Jun Wang, Xiaoguang Xu

Department of Earth and Atmospheric Sciences, University of Nebraska Lincoln
Lincoln, Nebraska, USA, 68516

Correspondence to: J. Wang (jwang7@unl.edu)

Abstract. Theoretical analysis is conducted to reveal the information content of aerosol vertical profile in space-borne measurements of the backscattered radiance and degree of linear polarization (DOLP) in the O_2 A and B bands. Assuming a quasi-Gaussian shape for aerosol vertical profile characterized by peak height H and half width γ (at half maximum), the Unified Linearized Vector Radiative Transfer Model (UNL-VRTM) is used to simulate the Stokes 4-vector elements of upwelling radiation at the top of atmosphere (TOA) and their Jacobians with respect to H and γ. Calculations for different aerosol types and different combinations of H and γ values show that the wide range of gas absorption optical depth in O_2 A and B band enables the sensitivity of backscattered DOLP and radiance at TOA to the aerosol layer at different altitudes. Quantitatively, DOLP in O_2 A and B bands is found to be more sensitive to H and γ than radiance, especially over the bright surfaces (with large visible reflectance). In many O_2 absorption wavelengths, Degree of Freedom for Signal (DFS) for retrieving H (or γ) generally increases with H (and γ) and can be close to unity in many cases, assuming that the composite uncertainty from surface and aerosol scattering properties as well as measurements is less than 5%. Further analysis demonstrates that DFS needed for simultaneous retrieval of H and γ for high-lofted aerosol profiles (H > 2 km) can be obtained from a combined use of DOLP measurements at ~10 O_2 A and B absorption wavelengths. However, challenges still remain for resolving aerosol profiles with H less than 2 km. Future

Atmos. Meas. Tech. Discuss., doi:10.5194/amt-2015-340, 2016
Manuscript under review for journal Atmos. Meas. Tech.
Published: 18 January 2016

Atmospheric Measurement Techniques Discussions

hyperspectral measurements of DOPL in O_2 A and B bands are needed to continue studying their potential and their combination with radiance and DOPL in atmospheric window channels for retrieving the vertical profiles of aerosols, especially highly scattering aerosols, over land.

Key words: remote sensing, aerosol, degree of linear polarization, O_2 A and B band, Degree of Freedom for Signal

Atmos. Meas. Tech. Discuss., doi:10.5194/amt-2015-340, 2016
Manuscript under review for journal Atmos. Meas. Tech.
Published: 18 January 2016

Atmospheric Measurement Techniques Discussions

1. Introduction

Aerosols are ubiquitous in the atmosphere and play an important role in the climate system through their direct effects on the transfer of radiative energy (Forster et al., 2007) and indirect effects on cloud microphysical properties by serving as cloud condensation nuclei (Twomey, 1977), which is one of the largest uncertainty sources to estimate and interpret the Earth's changing energy budget (IPCC, 2014). These climate effects of aerosols are highly sensitive to the variation of aerosol optical and physical properties, not only in the horizontal but also in the vertical dimension. Information on aerosol vertical distribution is essential for providing a clear description of aerosol transport processes (Colarco et al., 2004), as well as for understanding how radiative energy and clouds in the atmosphere are affected by aerosols (Wang et al., 2004; 2009). Consequently, the vertical distribution of aerosols affects the sign and magnitude of regional temperature change due to global warming (Haywood and Shine, 1997; Meloni et al., 2005; Zarzycki and Bond, 2010; Samset and Myhre, 2011; Samset et al., 2013), the precipitation patterns (Huang et al., 2009), and air quality and visibility (Liu, et al., 2011; Kessner et al., 2013).

Because aerosols are highly variable in space and time, the only way to obtain the information of aerosol vertical distribution on a global scale is by means of satellite remote sensing. Using lidar, such as the Cloud-Aerosol Lidar Infrared Pathfinder Satellite Observations (CALIPSO) (Vaughan et al., 2004; Hunt et al., 2009), is a direct method to probe the vertical structure of aerosols in cloud-free conditions. However, the active remote sensing of aerosols with lidar is expensive and its narrow swath limits the spatial coverage. For example, CALIPSO flies over a given site only once every 16 days (Winker, 2003). Most passive satellite-based measurements in ultraviolet and/or visible bands, such as those from the Multi-angle Imaging SpectroRadiometer (MISR), the Ozone Monitoring Instrument (OMI) (Levelt et al.,

Atmos. Meas. Tech. Discuss., doi:10.5194/amt-2015-340, 2016
Manuscript under review for journal Atmos. Meas. Tech.
Published: 18 January 2016

Atmospheric Measurement Techniques Discussions

2006), and the Polarization and Directionality of the Earth's Reflectance (POLDER) (Deschamps et al., 1994; Tanré et al., 2011), contain limited vertical information of aerosols beyond the aerosol optical depth (AOD), a columnar quantity. Only with additional constraints (such as aerosol single scattering albedo and AOD) from independent sources, can OMI measurements be used to derive the centroid height of a highly elevated absorbing aerosol layer (Satheesh et al., 2009). It is also noted that multi-angle instrument such as MISR can be used to derive the stereo height of an aerosol layer, although such derivation is not based on the particle scattering and radiative transfer calculations (Kahn et al., 2007).

In the last decade, various studies have proposed methods for the passive remote sensing of aerosol vertical profile from space using measurements in the O_2 A band, such as those from the Global Ozone Monitoring Experiment (GOME) (Koppers and Murtagh, 1997) and the SCanning Imaging Absorption spectroMeter for Atmospheric CHartographY (SCIAMACHY) (Corradini and Cervino, 2006; Sanghavi et al., 2012). The underlying fundament physical principle is that O_2 is a well-mixed gas in the atmosphere with well-defined vertical structure, and hence, assuming other factors being equal, the change in the amount of upwelling radiation in the O_2 *A* band contains information about how aerosol particles affect O_2 *A* absorption through multiple scattering in different altitudes. Indeed, this idea dates back to Hanel (1961) and Yamamoto and Wark (1961) who are among the first to study the retrieval of cloud top pressure from reflection spectra in the O_2 A band, although cloud particles are larger and more efficient in scattering, and therefore, have bigger impact on radiative transfer in the O_2 A band than aerosol particles. Following their pioneer work, a wealth of literatures have developed and evaluated the techniques to retrieve cloud top height from O_2 A band in the last four decades (Grechko et al., 1973; Mitchell and O'Brien, 1987; Fischer and Grassl, 1991; Fischer et al., 1991; O'Brien and Mitchell, 1992;

Atmos. Meas. Tech. Discuss., doi:10.5194/amt-2015-340, 2016
Manuscript under review for journal Atmos. Meas. Tech.
Published: 18 January 2016

Atmospheric Measurement Techniques Discussions

Harrison and Min, 1997; Pfeilsticker et al., 1998). In contrast, studies on the feasibility of retrieving aerosol vertical profile form O_2 A band were conducted primarily in the last decade (Heidinger and Stephens, 2000; Min et al., 2004; van Diedenhoven et al., 2007; Kokhanovsky and Rozanov, 2004; Daniel et al., 2003, Sanghavi et al., 2012; Corradini and Cervino, 2006; Koppers and Murtagh, 1997; Dubuisson et al., 2009). These studies showed that the radiance at the top-of-atmosphere in the O_2 A band contain information on the vertical structure of aerosol scattering, and this information can only be retrieved in clear skies over sufficiently dark surfaces such as ocean away from glint. Hence, retrieving aerosol profiles over land still remains a challenge because land surface reflectance is often much higher in the O_2 A band than in the ultraviolet and blue wavelengths.

The objective of this study is to systematically study the information content of aerosol vertical profile from a combined use of polarization and radiance measurements in the O_2 A and B bands. The underlying motivation is that the surface polarized reflectance is generally low (Maignan et al., 2009) and hence, using polarization in O_2 A and B bands may provide a unique opportunity to retrieve aerosol vertical profile over not only dark but also bright surfaces (such as desert and urban regions). Stam et al. (1999) investigated the linear degree of polarization (DOLP) of reflected and transmitted light in the O_2 A band for a few typical atmospheric profiles and identified different regimes of DOLP based on the gas absorption optical depth. Aben et al. (1999) presented that the polarization measurements in the O_2 A band in clear sky contain rich spectral fine-structure. This fine structure is shown to contain information of vertical distribution of aerosols by various modeling studies (Preusker et al., 1995; Boesche et al., 2006, 2009; and Zeng et al. 2008). Most recently, Wang et al. (2014) showed that the DOLP in the O_2 A band has higher sensitivity to the vertical profile of aerosols than that of intensity, especially over the high

Atmos. Meas. Tech. Discuss., doi:10.5194/amt-2015-340, 2016
Manuscript under review for journal Atmos. Meas. Tech.
Published: 18 January 2016

Atmospheric Measurement Techniques Discussions

reflective surface. In this study, we carry out further sensitivity studies to assess the potential for retrieving aerosol vertical profile by considering the polarization in both O_2 A and B bands. With the recent deployment of such wide-swath satellite sensors as Earth Polychromatic Imaging Camera (EPIC) on Deep Space Climate Observatory (DSCOVR) that has a channel to measure radiance in O_2 A band, http://epic.gsfc.nasa.gov/epic.html), as well as the development of future science missions such as Pre-Aerosol, Clouds, and ocean Ecosystem (PACE) that may have the opportunity to have a polarimeter, http://decadal.gsfc.nasa.gov/pace-resources.html), it is essential to evaluate the use of O_2 A and O_2 B bands for retrieving aerosol vertical profile.

Our study here differs from the past studies in twofold. First, to investigate the effects of various aerosols on DOLP at hyperspectral resolution under different surface conditions, we not only focus on the analysis in the O_2 A, but also extend the analysis to include the O_2 B band. We note that Sanghavi et al. (2012) and Vasilkov et al. (2013) have demonstrated the potential of radiance in O_2 A and B for retrieving aerosol profile over dark surfaces, but the potential of using both radiance and DOPL in O_2 A and O_2 B remains uninvestigated. Second, our analysis of information content is conducted to recommend the most informative channels for the design of future sensors that will measure the polarization in O_2 A and B bands. This recommendation is needed because: (a) few satellite sensors measure the state of polarization in O_2 A and B bands at hyperspectral resolution with an aim for retrieving aerosols, although a Fouries Transform Spectrometer (TANSO-FTS) carried on Japanese Greenhouse Gases Observing Satellite (GOSAT) is capable to measure highspectral resolution two-orthogonal polarizations in O_2 A band (Kuze et al., 2009); (b) existing routine measurements of polarization spectra in O_2 A band taken by polarimetric instruments (such as those aboard on GOME-2 and SCIAMACHY) are primarily used to

Atmos. Meas. Tech. Discuss., doi:10.5194/amt-2015-340, 2016
Manuscript under review for journal Atmos. Meas. Tech.
Published: 18 January 2016

Atmospheric Measurement Techniques Discussions

improve radiometric calibration. We note that satellite spectrometers such as GOME-2, SCIAMACHY, and GOSAT have a large number of spectral samplings, but not all of them are necessary for operational retrievals. Hence, under cost constraints, if we want to measure polarization in both O_2 A and B bands with a wide spatial coverage and resolution (unlike GOSAT with narrow swath or GOME-2 with big footprint), it is important to answer the question: at which spectra should these measurements be taken to maximize the information content for aerosol vertical distribution?

To this end, we first will use a rigorous radiative transfer model, the Unified Linearized Vector Radiative Transfer Model (UNL-VRTM) (Wang et al., 2014) to simulate the Stokes elements and their Jacobians with respect to the aerosol optical and physical parameters, in both O_2 A and B bands at hyperspectral resolution. Subsequently, the analysis of information content is conducted at hyperspectral resolution based on the optimal estimation theory (Rodgers, 2000), which allows us to identify the most useful channels for retrieving the aerosol vertical profile. We use the Degree of Freedom for Signal (DFS) to describe the sensitivities of individual wavelengths in both O_2 A and B bands to the aerosol vertical profile and select the combination of most sensitive wavelengths. DFS is a variable that can quantify the number of useful independent pieces of information in the measurement for retrieving corresponding parameter(s) of our interest (Rodgers, 2000).

In Section 2, we outline the theoretical basis of this study including the introduction of UNL-VRTM and the optimization strategy used for the information content analysis. In Section 3, we discuss the sensitivities of DOLP and intensity in both O_2 A and B bands to the aerosol profiles in terms of DFS, and present the results about the potential of retrieving the aerosol vertical profile (aerosol peak height and

Atmos. Meas. Tech. Discuss., doi:10.5194/amt-2015-340, 2016
Manuscript under review for journal Atmos. Meas. Tech.
Published: 18 January 2016

Atmospheric Measurement Techniques Discussions

half width, simultaneously) with multiple channels in O_2 A and B bands. The summaries and conclusions follow in Section 4.

2. Description of Methods and Computations

2.1 Definition of DOLP

The degree of polarization (DOP) is a quantity that describes partially polarized light (Chandrasekhar, 1950). It is defined as the ratio between the intensity of the totally polarized component to the total intensity of the light:

$$DOP = \frac{\sqrt{Q^2+U^2+V^2}}{I} \quad (1)$$

where the Stokes parameter I describes the total intensity, Q and U the linear polarization and V the circular polarization of the light beam. Since the reflection of sunlight by natural surfaces and atmospheric scattering generate very weak elliptic polarization (Coulson, 1988), V is negligibly small compared to the other three parameters. The degree of linear polarization (DOLP) of light can be given as:

$$DOLP = \frac{\sqrt{Q^2+U^2}}{I} \quad (2)$$

For skylight measurements within the principal plane, $U = 0$. To preserve the sign of Q, the DOLP in principal plane can be written as (Hoverier et al, 2004):

$$DOLP = -\frac{Q}{I}. \quad (3)$$

2.2 Forward Radiative Transfer Model

Atmos. Meas. Tech. Discuss., doi:10.5194/amt-2015-340, 2016
Manuscript under review for journal Atmos. Meas. Tech.
Published: 18 January 2016

Atmospheric Measurement Techniques Discussions

A numerical testbed, the Unified Linearized Vector Radiative Transfer Model (UNL-VRTM) (Wang et al., 2014), is used in the present study. The UNL-VRTM comprises the following several modules: (1) a linearized vector radiative transfer model (VLIDORT, Spurr, 2006), which computes simultaneously the Stokes 4-vector elements and their Jacobians with respect to various atmospheric and surface properties (Spurr et al., 2008), including aerosol single scattering properties at different layers and as a column, as well as the aerosol height (Wang et al., 2014); (2) a linearized Mie scattering code (Spurr et al., 2012), which computes the optical properties of spherical aerosol particles and their Jacobians with respect to aerosol physical parameters such as refractive index and particle size distribution; (3) a linearized T-matrix electromagnetic scattering code (Spurr et al., 2012), which is same as (2), but for nonspherical aerosols; (4) a surface bi-directional reflectance (BRDF) and polarization function (BPDF) module (Spurr, 2004), which provides surface BRDF and the Jacobians with respect to kernel parameters. (5) a module that computes Rayleigh scattering and gas absorption with HITRAN database (Rothman et al., 2013), which calculate the optical thickness of atmospheric molecule scattering and absorption, respectively. Wang et al. (2014) has validated the calculations of Jacobians of [I, Q, U] with respect to the aerosol physical parameters such as refractive index, particle size distribution, and aerosol height. With UNL-VRMT, Xu and Wang (2015) and Xu et al. (2015) studied the information content of the ground-based photopolarimetric measurements of sky light and developed an algorithm for the retrieval of fine-mode and coarse-mode aerosol microphysical parameters.

2.3 Aerosol Vertical Profile

Atmos. Meas. Tech. Discuss., doi:10.5194/amt-2015-340, 2016
Manuscript under review for journal Atmos. Meas. Tech.
Published: 18 January 2016

Atmospheric Measurement Techniques Discussions

Various shapes of aerosol vertical profile can be defined in UNL-VRTM including uniform, exponentially-decreasing, and quasi-Gaussian shapes. Since our main purpose is to study the sensitivity of the degree of polarization and intensity to aerosol vertical distribution, we select the quasi-Gaussian profile (Spurr and Christi, 2014). The optical depth profile is given by

$$\tau_A(z) = C\frac{\exp\left(-h\left|z-H_{\text{peak}}\right|\right)}{\left[1+\exp\left(-h\left|z-H_{\text{peak}}\right|\right)\right]^2} \quad (4)$$

where C is a constant related to the total optical depth, h is related to the half width (γ) at the half maximum (of AOD), which is defined as $\gamma = \frac{\ln(3+\sqrt{8})}{h}$. H_{peak} is the peak height or the altitude at which AOD is the largest.

2.4 Information Content and Degree of Freedom for Signal (DFS)

The relationship between the measurement vector $\mathbf{y}$ (such as DOLP and intensity in O_2 A band) and the state vector $\mathbf{x}$ (such as aerosol parameters and aerosol vertical profile) to be retrieved can be given by

$$\mathbf{y} = \mathbf{F}(\mathbf{x}) + \boldsymbol{\varepsilon} \quad (5)$$

where $\mathbf{F}(\mathbf{x})$ is a forward model and $\boldsymbol{\varepsilon}$ is the measurement error.

For the purpose of examining the information content of a measurement, it is convenient to consider a linear problem, or divide a non-linear process into linear sub-processes. A linearization of the forward model at a reference state $\mathbf{x}_0$ will be adequate for this purpose, provide that $\mathbf{F}(\mathbf{x})$ is linear within the error bounds of the retrieval:

Atmos. Meas. Tech. Discuss., doi:10.5194/amt-2015-340, 2016
Manuscript under review for journal Atmos. Meas. Tech.
Published: 18 January 2016

Atmospheric Measurement Techniques Discussions

$$\mathbf{y} - \mathbf{F}(\mathbf{x}_0) = \frac{\partial \mathbf{F}(\mathbf{x})}{\partial \mathbf{x}}(\mathbf{x} - \mathbf{x}_0) + \boldsymbol{\varepsilon} = \mathbf{K}(\mathbf{x} - \mathbf{x}_0) + \boldsymbol{\varepsilon} \quad (6)$$

where $\mathbf{x}_0$ defines a linearization point or the *a priori* information. With the Bayesian approach assuming Gaussian distribution for measurement and a priori errors, Rodgers (2000) showed that the retrieval uncertainty (the *a posteriori* covariance matrix **S**) is relevant to the Jacobian **K**:

$$\mathbf{S}^{-1} = \mathbf{K}^{\mathbf{T}}\mathbf{S}_{\boldsymbol{\varepsilon}}^{-1}\mathbf{K} + \mathbf{S}_{\mathrm{a}}^{-1}, \quad (7)$$

where $\boldsymbol{S}_{\boldsymbol{\epsilon}}$ is the measurement error covariance matrix and $\mathbf{S}_{\mathrm{a}}$ is the *a priori* error covariance matrix. To obtain the link between the retrieval and the true state, the averaging kernel matrix **A** is introduced, which is defined as:

$$\boldsymbol{A} = (\boldsymbol{K}^{\boldsymbol{T}}\boldsymbol{S}_{\boldsymbol{\varepsilon}}^{-\mathbf{1}}\boldsymbol{K} + \boldsymbol{S}_{\boldsymbol{a}}^{-\mathbf{1}})^{-\mathbf{1}}\boldsymbol{K}^{\boldsymbol{T}}\boldsymbol{S}_{\boldsymbol{\varepsilon}}^{-\mathbf{1}} \quad (8)$$

The trace of **A** is called the degree of freedom for signal (DFS), which describes the number of useful independent pieces of information in the measurement for the retrieval, and hence is a measure of information content to infer a posteriori state vector. For each single retrieval variable, the value of DFS is between 0 and 1. If DFS for one aerosol parameter is close to 0, it indicates that the measurements have no information for the retrieval of that parameter. In our following sensitivity study, the measurement error is assumed to be 0.05 by following Xu and Wang (2015) and the *a priori* error is assumed to be 100% for both aerosol peak height and half width.

2.5 Design of Sensitivity Experiments

Atmos. Meas. Tech. Discuss., doi:10.5194/amt-2015-340, 2016
Manuscript under review for journal Atmos. Meas. Tech.
Published: 18 January 2016

Atmospheric Measurement Techniques Discussions

Three types of experiment are conducted: (a) the sensitivity of DOLP and radiance of scattered sunlight at the top of atmosphere to the aerosol peak height H over various surface types, assuming γ (the half width at half maximum) is well known; (b) the sensitivity of DOLP and radiance γ over various surface conditions, assuming that the aerosol peak height is well known, and (c) the sensitivity of DOLP and radiance to both H and γ. We conducted these experiments for several types of aerosols listed in Table 1, i.e., strong absorbing (such as soot), moderate absorbing (such as dust), and strong scattering aerosols (such as sulfate). For the purpose of simplicity, we present results for moderate absorbing (dust) aerosols in detail. Results for other types of aerosols are highlighted as sensitivity analysis in the last part of the result section. In this paper, dust aerosols are assumed as spherical with lognormal size distribution having effective radius $r_{\text{eff}} = 1$ μm and effective variance $v_{\text{eff}} = 0.45$, and with refractive index 1.53-0.008i in the O_2 A and B bands. While ambient dust particles are often nonspherical, spherical dust particles or coarse-mode spherical particles were also observed in the atmosphere (Wang et al., 2003). Our treatment of dust particles as spherical is not ideal, and this non-ideality is primarily due to the difficulties of linearized T-matrix technique for computing scattering properties of large particles (Wang et al., 2014; Xu and Wang, 2015). While other techniques for computing scattering properties of non-spherical particles are promising, their corresponding numerical codes have not been linearized so far.

The information content of measurements in each experiment is characterized in terms of DFS for O_2 A, O_2 B and combined O_2 A and O_2 B bands. Each experiment is also carried out for a set of different aerosol profiles in which the aerosol peak heights are assumed to range from 1 to 16 km with increment of 1 km and the aerosol half width is assumed to be 0.25 to 4 km with increment of 0.25 km. All the simulations are conducted at the spectral resolution of 0.01 nm.

Atmos. Meas. Tech. Discuss., doi:10.5194/amt-2015-340, 2016
Manuscript under review for journal Atmos. Meas. Tech.
Published: 18 January 2016

Atmospheric Measurement Techniques Discussions

3. Results

3.1 Gas Absorption Optical Depth in O_2 A and B Bands

O_2 has two strong absorption bands in the 755–775 nm and 685–695 nm, which are called O_2 A and B bands, respectively. Figures 1 a–b show the spectral absorption optical depth in these two bands for a typical mid-latitude summer atmosphere (McClatchey et al., 1972). The maximum absorption optical depth can reach 100 and 7 in the O_2 A and B bands, respectively. Therefore, the sunlight can be fully attenuated before it reaches the surface at wavelengths of strong O_2 absorption. The large variability of absorption optical depth in the O_2 A and B bands enables sunlight from the top-of-atmosphere (TOA) to penetrate the atmosphere at different depths (before it completely attenuated in the atmosphere, Figure 1 c-d). For instance, the penetration altitude is about 30 km above the surface in the center of O2 A band, and decreases to 20 km, 10 km, and near the surface as the wavelength moves from the center to the edge of O_2 *A* band (Figure 1c). Similarly, for wavelengths at the O_2 *B* band, the penetration altitude can vary from 15 km to the surface depending on the wavelength (Figure 1d). Hence, the spectral contrast of reflected sunlight in terms of their intensity and polarization contains information of atmospheric scattering (including aerosol scattering) at different altitudes of the atmosphere (Figure 1 e-f).

Considering that the absorption optical depth highly varies with wavelength in both O_2 A and B bands, we plot in Figures 1 e–f the DOLP at the top of an *aerosol-free* atmosphere over various surface types (with reflectance from 0.05, 0.2 to 0.5) as a function of molecular absorption optical depth. It should be noted that the O_2 absorption is much larger than the Rayleigh scattering optical depth in both bands.

Atmos. Meas. Tech. Discuss., doi:10.5194/amt-2015-340, 2016
Manuscript under review for journal Atmos. Meas. Tech.
Published: 18 January 2016

Atmospheric Measurement Techniques Discussions

As shown in Figures 1 e–f, the magnitude of O_2 absorption optical depth can be categorized into three distinct regions.

- The first region has the gaseous absorption optical depth less than 0.1. Because of the strong interaction between atmospheric scattering and surface reflection, DOLP is less than 20% when absorption optical depth is very small (for example << 0.1) in Figures 1 e –f. As surface reflectance increases from 0.05 (red line) to 0.2 (green line), the DOLP decreases because the stronger multiple scattering occurring between the surface and atmosphere decreases the DOLP. Indeed, DOLP is nearly zero when surface reflectance is 0.5.
- The second region has the gaseous absorption optical depth larger than 20. The DOLP in this region is mainly determined by scattering in the upper atmospheric layer where molecular scattering dominates and leads to larger DOLP regardless of the surface reflectance, since the incident solar light cannot reach lower altitude and light scattered in the lower atmosphere cannot easily reach the TOA (because of strong O_2 absorption).
- The third region is located between the above defined first and second regions. In this region, light can penetrate through and be reflected by the lower atmosphere (and surface depending on absorption optical depth), and thus intensity and polarization of the upwelling radiation at TOA has the sensitivity to the vertical distribution of scattering in the whole atmospheric column.

3.2 Sensitivity of *DOLP* to the Aerosol Vertical Distribution

Atmos. Meas. Tech. Discuss., doi:10.5194/amt-2015-340, 2016
Manuscript under review for journal Atmos. Meas. Tech.
Published: 18 January 2016

Atmospheric Measurement Techniques Discussions

To investigate the sensitivity of DOLP and intensity to aerosol vertical distribution, we focus mainly on two parameters, the aerosol peak height (H) and half width (γ) at half maximum, which are essential to determine the aerosol vertical profile as mentioned in the previous section.

To explain the physics underlying the results, we first present the results for four different aerosol profiles (Figure 2a) in which the aerosol peak height H varies from 4 to 13 km with an increment of 3 km. Here, the column aerosol optical depth is assumed to be 0.2 and γ is 2 km. Figure 2b shows the differences of DOLP (ΔDOLP) from one wavelength (760 nm) within the O_2 A band to the nearby continuum band (757 nm) for surface reflectance of 0.0, 0.05 and 0.2. The solar zenith angle and view zenith angle are 66° and 0°, respectively. It can be seen that ΔDOLP decreases as the surface reflectance increases, which is caused by strengthened surface depolarization and increased multiple scattering. In addition, it can be seen that ΔDOLP also decreases as the aerosol peak height increases for a given surface reflectance (Figure 2b). While the DOLP of Rayleigh scattering is positive and strong, the DOLP of spherical aerosols is negative and weaker compared to that of Rayleigh scattering. Consequently, the increase of scattering by aerosols, as aerosol gets aloft, can partially offset the effects of Rayleigh scattering, resulting in less positive DOLP (Wang et al., 2014). It is noted that the lower the aerosol layer, the increased absorption in O_2 A band suppresses the aerosol scattering. This explains the increase of DOLP in the O_2 A band as the aerosol peak height decreases (closer to the surface). The same patterns can also be seen in the O_2 B band (Figure 2c). Also, it can be seen from this figure that the change of DOLP with respect to the aerosol peak height is sensitive to wavelength. Indeed, in some absorption wavelengths, the O_2 absorption optical depths can be sufficiently large (7.79 at 687.19 nm) that aerosols near the surface have much less chance to interact with the incident light. Thus, the DOLP differences at these wavelengths are more sensitive to

Atmos. Meas. Tech. Discuss., doi:10.5194/amt-2015-340, 2016
Manuscript under review for journal Atmos. Meas. Tech.
Published: 18 January 2016

Atmospheric Measurement Techniques Discussions

high-altitude aerosol layers (Figure 1c). However, at some other wavelengths, the O_2 absorption optical depths (such as 0.88 at 759.98 nm) are relatively smaller and the light can reach lower atmosphere. The DOLP differences at these wavelengths are more sensitive to low-altitude aerosol layers (Figure 1b).

Figure 2d is the profile of aerosol optical depth for different γ values, where H is 5 km and the column aerosol optical depth is assumed to be 0.2. Similar as Figures 2b–c, Figures 2e–f show that the ΔDOLP for various γ values (with the same H). Consistent with Figures 2b and 2c, ΔDOLP decreases as the surface reflectance increases. Also, it can be seen that for given surface reflectance, as γ increases, ΔDOLP decreases. Because O_2 absorption coefficient above the aerosol peak height is smaller than that below the aerosol peak height, the elevated portion of aerosols above the peak height (due to the increase of profile half width) have a larger effect on DOLP than the counterpart below the aerosol peak height, counteracting more positive DOLP from Rayleigh scattering.

To further evaluate if the findings revealed in Figure 2 can be generalized, we compute the DOLP at 759.98 nm at TOA as a function of H and γ for different surface reflectance values (Figure 3). Top panels of Figure 3 show the DOLP at TOA for wavelength 759.98 nm as functions of H and γ for three different surface reflectance values of 0.0, 0.2 and 0.5 at the scattering angle Θ=120° (a nadir view with solar zenith angle of 60°). Bottom panels correspond to scattering angle Θ=150°. These results confirm that: (a) an increase of surface albedo leads to decrease the DOLP at TOA, and (b) DOLP decreases as the peak height H increases for the same γ value. Moreover, these results also suggest that DOLP at TOA has a strong angular dependence. It can be seen that the DOLP at Θ=120° is positive for all chosen H and γ. The maximum of DOLP at TOA occurs when aerosols appear in the near surface. In contrast, DOLP

Atmos. Meas. Tech. Discuss., doi:10.5194/amt-2015-340, 2016
Manuscript under review for journal Atmos. Meas. Tech.
Published: 18 January 2016

Atmospheric Measurement Techniques Discussions

at Θ=150° is found to be negative for all combinations of aerosol peak height and half width (bottom three panels in Figure 3). This contrast can be explained by the different angular dependence of DOLP between Rayleigh scattering and aerosol scattering. As discussed in Wang et al. (2014), the DOLP of Rayleigh scattering (Fig. 8 in Wang et al., 2014) is positive at all scattering angles (with peak value at Θ=90° and zero at Θ=180°); aerosol particles often yield negative DOLP at all backscattering angles, with the largest negative DOLP at around Θ=150°. Regardless of angle, however, it is expected that the increase of aloft aerosol scattering, either through increase of peak height or through increase of half width or both, can lead to a decrease of DOLP for the same surface reflectance (Figure 3).

3.4 Calculation of the DFSs

The actual observations inevitably contain instrumental error and measurement noise. It is critical to properly treat these experimental errors in the design of retrieval methods. In the following analysis we assume that aerosol properties including optical depth are known with some uncertainties, and the only parameters to be retrieved are related to aerosol vertical profile. Hence, the measurement errors defined here also include the model errors.

To compare the information content of the DOLP and intensity at TOA for retrieving aerosol vertical distribution, we calculate the DFSs for aerosol peak height *H* at each individual wavelength using: (a) only radiances in O_2 A band, (b) only DOLP in O_2 A band, and (c) only DOLPs in the O_2 B band. It can be seen that in Figure 4(a), the maximum DFS for using radiance only is about 0.35 at the wavelength near 759.7 nm in the O_2 A band. However, the DFSs for using DOLPs are often larger than 0.4, with maxima values close to unity, in both O_2 A (Figure 4b) and O_2 B bands (Figure 4c). Figure 4 hence

Atmos. Meas. Tech. Discuss., doi:10.5194/amt-2015-340, 2016
Manuscript under review for journal Atmos. Meas. Tech.
Published: 18 January 2016

Atmospheric Measurement Techniques Discussions

suggests that the polarization of light contains more information on the aerosol peak height than that of intensity.

The DFS values in Figures 4 d–f are sorted in descending order for three cases in Figures 4 (a), (b), and (c), respectively. The x-axis in Figures 4 d–f indicates the number of spectral wavelengths (or channels). The left-side y-axis indicates DFSs and the right-side y-axis represents the corresponding gaseous absorption optical depth for an individual wavelength. As shown in Figure 4 d, the gaseous absorption optical depths corresponding to the first ten maximum DFSs of radiance in the O_2 A band are above 5.0. In contrast, the counterparts for the DFSs of DOLP in O_2 A and B bands are above 1.0 and 0.35, respectively (see Figures 4 e and f). Furthermore, there are no less than 10 wavelengths (simulated at 0.01-nm interval) having DFS values close to 1 in DOLP measurements in both O_2 A and B bands; but the DFS values of radiance measurements are always below 0.4. These findings from Figure 4 further suggest that DOLP can have more information content for inferring aerosol peak height H than intensity.

Figure 5 shows the DFS in DOLP measurements for inferring aerosol peak height H as a function of aerosol peak height H and half width at half maximum γ for three wavelengths in both O_2 A and B bands for different surface reflectance values, 0.0, 0.2 and 0.5. We can find that, at some wavelengths where the O_2 absorption optical depths are smaller relatively (such as 759.98 nm with optical depth of 0.88), the DFS values are more influenced by the change of surface reflectance than at other wavelengths where the O_2 absorption optical depths are larger (such as 762.68 nm with optical depth of 2.7). Indeed, DFS approaches zero at 762.68 nm for aerosol peak height less than 2 km. For the same wavelength (e.g.,

Atmos. Meas. Tech. Discuss., doi:10.5194/amt-2015-340, 2016
Manuscript under review for journal Atmos. Meas. Tech.
Published: 18 January 2016

Atmospheric Measurement Techniques Discussions

each row in Figure 6), DFS values decrease as the surface reflectance increases; for surface reflectance of 0.5, the DFS is less than 0.5 for aerosol peak height H below 2 km, regardless of γ.

Similarly, we calculate the DFS in DOLP measurements for γ (Figure 6). It can be seen that although the DFS values are not as sensitive to the change of surface reflectance as that shown in Figure 5 for inferring aerosol peak height, they have remarkable spectral dependence. At some wavelengths such as 759.98 and 689.78 nm, the DFS values for γ are larger (than 0.5) for low-level aerosol layer H below 2 km except for γ less than 1 km; however, at other wavelengths such as 762.68 nm, the DFS values γ for are more sensitive to higher aerosol layer.

The question arises: can the two pieces of information for aerosol vertical profile (e.g., peak height and half width) be retrieved from combined use of several different wavelengths in both O_2 A and B bands? To address this question, we select the most informative channels sequentially following Rodgers (1996). We first sorted DFS values in DOLP measurements at each wavelength in a descending order in both O_2 A and B bands for a baseline aerosol vertical distribution with peak height H of 8 km, half width at half maximum of 2 km, and surface reflectance of 0.2. The first channel is selected with the maximum DFS for H. Subsequently, DFSs are examined for a combination of the first channel to any of the rest channels, and the second channel is identified when the largest DFS value is achieved. More channels are further selected with the same process applied and thereby, each additional channel leads to the increase of DFS values at the possibly largest increasing rate.

Figure 7a shows the DFSs of the first channel DOLP in the O_2 A band for the retrieval of aerosol peak height H (e.g., 764.76 nm, the channel that maximizes DFS for the baseline vertical profile) as a

Atmos. Meas. Tech. Discuss., doi:10.5194/amt-2015-340, 2016
Manuscript under review for journal Atmos. Meas. Tech.
Published: 18 January 2016

Atmospheric Measurement Techniques Discussions

function of various combinations of H and γ values. It reveals that aerosol peak height H can be easily retrieved by using the first channel (regardless of γ values), given other aerosol parameters well characterized, for those aerosol layers higher than 5.5 km. However, DFS decreases rapidly and is nearly zero when most aerosols start to concentrate near the surface (e.g., as H and γ values approaches from 4 km to zero, or approach to the bottom corner of the panel of Figure 7a). As expected, DFS value for H increases as more channels are used (from 2, 4, 8, 16, to 32 shown in Figure 7 b–f), especially when aerosol layer is close the surface. For example, the white zone with zero DFS in the bottom left corner in Figure 8a is slowly filled up with colors of DFS > 0.1 from Figure 7b– f. Even with 32 channels, however, DFS is still smaller than 0.4 when H is smaller than 2 km (Figure 7f). Therefore, a greater number of channels or better DOLP accuracy are required to gain a sufficient signal for retrieving aerosol distribution below the boundary layer.

Similar to Figure 7, we calculated the DFS values for γ for a different number of channels in O_2 A and B bands and the results are presented in Figure 8. The pattern of DFS in Figure 8 is different from that in Figure 7; Figure 8 has the maxima of DFS in the bottom right corner of each panel while the latter has the maxima of DFS on the top. In other words, for larger H, DOLP has less sensitivity to large γ. Regardless, the physics remains the same; DFS increases when there are more aerosols in the upper layer (e.g., either lager H or larger γ width or both). As shown in Figure 8, we can find that using 32 channels can well retrieve γ for most possible vertical distributions of aerosols, except when aerosols present within a low-altitude thin layer or highly aloft.

Atmos. Meas. Tech. Discuss., doi:10.5194/amt-2015-340, 2016
Manuscript under review for journal Atmos. Meas. Tech.
Published: 18 January 2016

After we calculated the DFS values for single parameter of aerosol vertical distribution (either H or γ, respectively) for various number of selected channels, we calculated the DFS values in DOLP measurements from various selected channels in the O_2 A band for retrieving H and γ simultaneously. Figure 9 shows these DFS values as a function of H and γ. As we can see from Figure 9, the retrievable regions are very limited if only a few number of channels (< 8) are used. However, with more channels used, DFS values can approach to 2 when aerosol peaks in middle troposphere with large γ values. As shown in Figure 9f, when 64 wavelengths are used to retrieve H and γ values simultaneously, the retrievable regions cover most possible vertical distributions of aerosols, except for aerosols near the surface or aerosols within a very thin layer (e.g., γ less than 1 km).

Figure 10 shows the DFS values for simultaneously retrieving H and γ with the DOLP in (a) O_2 A band, (b) O_2 B band, and (c) the combination of A and B bands. It is evident that the combined use of O_2 A and B bands (Figure 10c) can significantly enhances the information content compared to the use of only the A (Figure 10a) or B band (Figure 10b) and can decrease the number of required channels for a sufficiently accurate retrieval. Figure 10c shows that 10 channels from O_2 A and B bands, as listed in Table 2, are sufficient to resolve H and γ for the cases studied (where H and γ are assumed to be 5.0 and 2.0 km, respectively).

The results presented above are based on the calculations that assume spherical dust particles. As a comparison, we also investigate other types of aerosols listed in Table 1, including soot (absorbing) and sulfate (non-absorbing) aerosols. Figure 11 shows the comparison of the DOLP at TOA and their corresponding DFS values for three types of aerosols, dust, sulfate and soot, as a functions of aerosol

Atmos. Meas. Tech. Discuss., doi:10.5194/amt-2015-340, 2016
Manuscript under review for journal Atmos. Meas. Tech.
Published: 18 January 2016

Atmospheric Measurement Techniques Discussions

peak height and half width at the scattering angle 120°. The wavelength is 760 nm. The figure shows that more absorbing aerosols (such as soot, Figure 11c) can lead to a smaller decrease of DOLP (or larger DOLP) as compared to the counterparts by less absorbing (such as dust, Figure 11a) and pure scattering aerosols (such as sulfate, Figure 11b); this can be understood because absorbing aerosols suppress the multiple scattering at the atmosphere. Correspondingly, the information content in DOLP (in terms of DFS values) are generally smaller for characterizing vertical profile of absorbing aerosols (as shown by the contrast between Figure 11f and Figure 11 d-e and the contrast between Figure 11i and Figure 11 g-h). However, while these difference of DFS exist between various type of aerosols because of their different physical and optical properties, the patterns of DFS variations generally appear the same regardless of aerosol type, all revealing that DFS is higher when aerosols are concentrated at high levels either due to larger H, larger γ, or both. Therefore, a combination of DOLP measurements in O_2 A and B bands enables the retrieval of aerosol vertical distribution for a wide-range of aerosol types.

4. Summary

In the present study, we carry out radiative transfer simulation in the O_2 A and B bands and explain the physics underlying the results. In order to identify the most sensitive spectral channels to the peak height and half width of aerosol vertical distribution, degree of freedom for signal (DFS) is used to examine the information contained in each individual wavelength in both O_2 bands. Our results show that the DOLP can have more information content for retrieving aerosols vertical distribution than intensity. The analysis suggests that, the DOLP at different wavelengths has different sensitivities to the aerosols at different altitudes. Our results also show that the combined use of DOLP in both the O_2 A and B bands can significantly enhance the information content and decrease the number of wavelengths needed for

Atmos. Meas. Tech. Discuss., doi:10.5194/amt-2015-340, 2016
Manuscript under review for journal Atmos. Meas. Tech.
Published: 18 January 2016

simultaneously retrieving aerosol peak height and vertical distribution than using only O_2 A or B band alone.

While a combined use of DOLP in O_2 A and B bands is shown to have great potential for characterizing the aerosol vertical profile from a passive remote sensing point of view, it is also shown to have difficulty in resolve aerosol vertical distribution below 2 km. Regardless, since aerosols within 2 km above the surface are normally well-mixed as a result of planetary boundary layer process, using DOLP in O_2 A and B bands to further detect and characterize the conditions where significant aerosol layers (including scattering aerosols) occur above the boundary layer over the land (including bright surfaces) can provide valuable supplements to the existing satellite observations for advancing our knowledge of aerosol 3D distribution in the atmosphere. For future studies, real measurements of DOPL in O_2 A and B bands are needed to further evaluate their potential as well as their combination with DOLP in atmospheric channels for retrieving aerosol profiles over land.

Acknowledgments:

Funding for this study was provided by the NASA Earth Science Division as part of GEO-CAPE mission study. J. Wang is grateful to Jassim (Jay) A. Al-Saadi for his support, and thanks the GEO-CAPE aerosol working group and science working group for their constructive suggestions and fruitful discussions. The Holland Computing Center of University of Nebraska – Lincoln and NASA High End Computing program are acknowledged for their help in computing.

Atmos. Meas. Tech. Discuss., doi:10.5194/amt-2015-340, 2016
Manuscript under review for journal Atmos. Meas. Tech.
Published: 18 January 2016

Atmospheric Measurement Techniques Discussions

References

Aben I. F., D. M. Helderman, and P. Stammes, 1999: Spectral fine-structure in the polarization of skylight, *Geophys. Res. Lett.* **26**. 591–594.

Boesche E., Stammes P., Ruhtz T., Preusker R., and Fischer J., 2006: Effect of aerosol microphysical properties on polarization of skylight: sensitivity study and measurements, *Appl. Optics*, 45, 8790–8805.

Boesche E., Stammes P., and Bennartz R., 2009: Aerosol influence on polarization and intensity in near-infrared O2 and CO2 absorption bands observed from space, *J. Quant. Spectrosc. Ra.*, 110, 223–239.

Colarco, P. R., M. R. Schoeberl, B. Doddridge, L. T. Marufu, O. Torres, and J. Welton, 2004: Transport of smoke from Canadian forest fires to the surface near Washington D.C.: Injection height entrainment and optical properties, *J. Geophys. Res*., 109. D06203, doi:10.1029/2003 JD004248.

Corradini, S. and Cervino, M., 2006: Aerosol extinction coefficient profile retrieval in the oxygen A band considering multiple scattering atmosphere Test case: SCIAMACHY nadir simulated measurements, *J. Quant. Spectrosc.. Ra.* 97, 354–380.

Coulson Kinsell L., 1988: Polarization and Intensity of Light in the Atmosphere. Hampton, Va. USA: A. Deepak Pub.

Daniel, J. S., S. Solomon, H. L. Miller, A. O. Langford, R. W. Portmann, and C. S. Eubank (2003), Retrieving cloud information from passive measurements of solar radiation absorbed by molecular oxygen and O2-O2, Journal of Geophysical Research, 108, 4515, doi:4510.1029/2002JD002994.

Atmos. Meas. Tech. Discuss., doi:10.5194/amt-2015-340, 2016
Manuscript under review for journal Atmos. Meas. Tech.
Published: 18 January 2016

Deschamps, P. Y., F. M. Breon, M. Leroy, A. Podaire, A., Bricaud. J. C. Buriez and G. Seze, 1994: The POLDER mission: Instrument characteristics and scientific objectives, IEEE, 32, 3, 598 - 615. DOI: 10.1109/36.297978.

Dubovik, O., Herman, M., Holdak, A., Lapyonok, T., Tanré, D., Deuzé, J. L., Ducos, F., Sinyuk, A., and Lopatin, A., 2011: Statistically optimized inversion algorithm for enhanced retrieval of aerosol properties from spectral multi-angle polarimetric satellite observations, *Atmos. Meas. Tech*., 4, 975-1018, doi:10.5194/amt-4-975-2011.

Dubuisson P., R. Frouin, D. Dessailly, L. Duforêt, J. F. Léon, K. Voss and D. Antoine, 2009: Estimating the altitude of aerosol plumes over the ocean from reflectance ratio measurements in the O2 A-band, *Remote Sensing of Environment*, 113, 1899-1911.

Fischer, J., Cordes, W., Schmitz-Peiffer, A., Renger, W., and Mörl, P., 1991: Detection of cloud-top height from backscattered radiances within the oxygen A band. Part 2: Measurements, J. Appl. Meteorol., 30, 1260–1267.

Fischer, J. and Grassl, H., 1991: Detection of cloud-top height from backscattered radiances within the oxygen A band. Part 1: Theoretical study, J. Appl. Meteorol., 30, 1245–1259.

Forster P., et al., 2007: Changes in atmospheric constituents and in radiative forcing. Climate Change 2007: The Physical Science Basis, S. Solomon et al. Eds., Cambridge University Press, 129–234.

Atmos. Meas. Tech. Discuss., doi:10.5194/amt-2015-340, 2016
Manuscript under review for journal Atmos. Meas. Tech.
Published: 18 January 2016

Grechko Y. I., V. I., Dianov-Klokov and I. P. Malkov, 1973: Aircraft measurements of photon paths in reflection and transmission of light by clouds in the 0.76 mm oxygen band, Atmos. Ocean Phys. 9, 262– 265.

Hanel R. A., 1961: Determination of Cloud Altitude from a Satellite, *J. Geophy. Res.*, 66, 4, DOI: 10.1029/JZ066i004p01300.

Harrison, L. and Min, Q., 1997: Photon Pathlengths from O2 A-band Absorption. IRS '96: Current Problems in Atmospheric Radiation. Proc. Intl. Rad. Symposium Fairbanks AK 19-24 Aug, 1996. A. Deepak Press, Hampton VA ISBN 0-937194-39-5, pp 594-598.

Haywood, J. M. and Shine, K. P., 1997: Multi-spectral calculations of the direct radiative forcing of tropospheric sulphate and soot aerosols using a column model. *Q. J. Roy. Meteorol. Soc.* **123**, 1907–1930.

Heidinger, A. K., and G. L. Stephens, 2000: Molecular line absorption in a scattering atmosphere. Part II: Application to remote sensing in the O2 A band. J. Atmos. Sci., 57, 1615–1634.

Hovenier J. W., van der Mee C, Domke H, 2004: Transfer of polarized light in planetary atmospheres. Kluwer.

Huang J., A. Adams, C. Wang and C. Zhang, 2009: Black carbon and West African monsoon precipitation: Observations and simulations. *Ann. Geophys*. 27, 4171–4181.

Hunt W. H., Winker D. M., Vaughan M. A., Powell K. A., Lucker P. L., and Weimer C., 2009: CALIPSO Lidar Description and Performance Assessment, *J. Atmos.Ocean. Tech.*, 26(7), 1214–1228.

IPCC, 2014: Climate Change 2014: Impacts, Adaptation, and Vulnerability. Part A: Global and Sectoral Aspects. Contribution of Working Group II to the Fifth Assessment Report of the Intergovernmental Panel on Climate Change [Field, C.B., V.R. Barros, D.J. Dokken, K.J. Mach, M.D. Mastrandrea, T.E. Bilir, M. Chatterjee, K.L. Ebi, Y.O. Estrada, R.C. Genova, B. Girma, E.S. Kissel, A.N. Levy, S. MacCracken, P.R. Mastrandrea, and L.L. White (eds.)]. Cambridge University Press, Cambridge, United Kingdom and New York, NY, USA, 1132 pp.

Kahn R. A., W.-H., Li, C. Moroney, D. J. Diner, J. V., Martonchik and E.. Fishbein, 2007: Aerosol source plume physical characteristics from space-based multiangle imaging, *J. Geophys. Res.*, *112*, D11205, doi:11210.11029/12006JD007647.

Kaufman, Y. J, Tanre, D., Boucher, O. A, 2002: Satellite view of aerosols in climate systems, *Nature*, 419:215–23.

Kessner, A., J. Wang, R. Levy and P. Colarco, 2013: Remote sensing of surface visibility from space: A look at the United States East Coast, *Atmos. Environ.,* 81, 136–147**.**

Kokhanovsky, A. A. and Rozanov, V. V., 2004: The physical parameterization of the top-of-atmosphere reflection function for a cloudy atmosphere–underlying surface system: the oxygen A-band case study, J. Quant. Spectrosc. Ra., 85, 35–55, doi:10.1016/S0022- 4073(03)00193-6.

Koppers, G. A. A. and Murtagh, D. P., 1997: Retrieval of height resolved aerosol optical thickness in the atmospheric band (Chapter 5), in: G.A.A. Koppers, Radiative transfer in the absorption bands of oxygen:

Atmos. Meas. Tech. Discuss., doi:10.5194/amt-2015-340, 2016
Manuscript under review for journal Atmos. Meas. Tech.
Published: 18 January 2016

Atmospheric Measurement Techniques Discussions

Studies of their significance in ozone chemistry and potential for aerosol remote sensing, Stockholm University, Stockholm, Sweden.

Kuze A., H. Suto, M. Nakajima and T. Hamazaki, 2009: Thermal and near infrared sensor for carbon observation Fourier-transform spectrometer on the Greenhouse Gases Observing Satellite for greenhouse gases monitoring. *Appl. Opt. vol.* 48, 35, pp. 6716-6733.

Levelt, P. F., G. H. J. van den Oord, M. R. Dobber, A. Ma¨lkki, H. Visser, J. de Vries, P. Stammes, J. Lundell, and H. Saari (2006), The Ozone Monitoring Instrument, IEEE Trans. Geosci. Remote Sens., 44(5), 1093 – 1101, doi:10.1109/TGRS.2006.872333**.**

Liu, Y., Z. Wang, J. Wang, E. J. Welton, R. A. Ferrare, R. K. Newson, 2011: The effect of aerosol vertical profiles on satellite-estimated surface particle sulfate concentrations *Remote Sensing of Environment*, 508-513.

Maignan, F., Breon, F. -M., Fedele, E., & Bouvier, M., 2009: Polarized refectances of natural surfaces: Spaceborne measurements and analytical modeling. Remote Sensing of Environment, 113, 2642−2650.

Meloni D., di Sarra A., Di Iorio T. and Fiocco, G., 2005: Influence of the vertical profile of Saharan dust on the visible direct radiative forcing. *J. Quant. Spectrosc. Radiat. Transfer.* **93**, 397–413.

Min, Q.L., Harrison, L. C., Kierdron, P., Berndt, J., and Joseph, E., 2004: A high-resolution oxygen A-band and water vapor band spectrometer, J. Geophys. Res., 109, D02202, doi:10.1029/2003JD003540.

Atmos. Meas. Tech. Discuss., doi:10.5194/amt-2015-340, 2016
Manuscript under review for journal Atmos. Meas. Tech.
Published: 18 January 2016

Atmospheric Measurement Techniques Discussions

Mishchenko, M. I. and Travis, L. D., 1997: Satellite retrieval of aerosol properties over the ocean using polarization as well as intensity of reflected sunlight, *J. Geophys. Res.,* 102, 16989–17013, doi:10.1029/96JD02425.

Mitchell, R. M. and O'Brien , D. M., 1987: Error estimates for passive satellite measurement of surface pressure using absorption in the A band of oxygen. *Journal of the Atmospheric Science*, 44, 1981-1990.

O'Brien, D. M. and R. M. Mitchell, 1992: Error estimates for retrieval of cloud-top pressure using absorption in the A-band of oxygen. *J. Appl. Meteor.* 31, 1179–1192.

Pfeilsticker, K., F. Erle, O. Funk, H. Veitel and U. Platt, 1998: First geometrical path lengths probability density function derivation of the skylight from spectroscopically highly resolving oxygen A-band observations. 1. Measurement technique atmospheric observations and model calculations, *J. Geophys. Res.* 103, 11483- 11504.

Preusker, R., U. Bottger, and J. Fischer, 1995: Spectral and bidirectional measurements of the Stokes vector in the O2 A band and their interpretation, In Atmospheric Sensing and Modeling II, (Ed Santer, R.P.) Proceedings of SPIE Vol. 2582, 13- 20.

Rodgers, C. D. 1996: Information content and optimisation of high spectral resolution measurements'. Pp. 136–147 in Optical spectroscopic techniques and instrumentation for atmospheric and space research II. SPIE, Volume 2830**.**

Rodgers, C. D., 2000: Inverse Methods for Atmospheric Sounding: Theory and Practice World Scientific Singapore.

Atmos. Meas. Tech. Discuss., doi:10.5194/amt-2015-340, 2016
Manuscript under review for journal Atmos. Meas. Tech.
Published: 18 January 2016

Atmospheric Measurement Techniques Discussions

Samset, B. H. and G. Myhre, 2011: Vertical dependence of black carbon sulphate and biomass burning aerosol radiative forcing *Geophys. Res. Lett.* 38, L24802, doi:10.1029/2011GL049697.

Samset, B. H., Myhre, G., Schulz, M., Balkanski, Y., Bauer, S., Berntsen, T. K., Bian, H., Bellouin, N., Diehl, T., Easter, R. C., Ghan, S. J., Iversen, T., Kinne, S., Kirkevåg, A., Lamarque, J.-F., Lin, G., Liu, X., Penner, J. E., Seland, Ø., Skeie, R. B., Stier, P., Takemura, T., Tsigaridis, K., and Zhang, K., 2013: Black carbon vertical profiles strongly affect its radiative forcing uncertainty, Atmos. Chem. Phys., 13, 2423-2434, doi:10.5194/acp-13-2423-2013.

Sanghavi, S., Martonchik, J. V., Landgraf J. and Platt U., 2012: Retrieval of the optical depth and vertical distribution of particulate scatterers in the atmosphere using O2A- and B-band SCIAMACHY observations over Kanpur: a case study, *Atmos. Meas. Tech.*, 5, 1099–1119, doi:10.5194/amt-5-1099-2012.

Satheesh, S. K., Torres, O., Remer, L. A., Babu, S. S., Vinoj, V., Eck, T. F., Kleidman, R. G., and Holben, B. N., 2009: Improved assessment of aerosol absorption using OMI-MODIS joint retrieval, J. Geophys. Res., 114, D05209, doi:10.1029/2008JD011024.

Spurr, Robert J. D., 2004: A new approach to the retrieval of surface properties from earthshine measurements. Journal of Quantitative Spectroscopy and Radiative Transfer, 83, 15−46**.**

Spurr, R. (2006), VLIDORT: A linearized pseudo-spherical vector discrete ordinate radiative transfer code for forward model and retrieval studies in multilayer multiple scattering media, *Journal of Quantitative Spectroscopy & Radiative Transfer*, *102*, 316-342.

Atmos. Meas. Tech. Discuss., doi:10.5194/amt-2015-340, 2016
Manuscript under review for journal Atmos. Meas. Tech.
Published: 18 January 2016

Atmospheric Measurement Techniques Discussions

Spurr, R., 2008: LIDORT and VLIDORT: Linearized pseudo-spherical scalar and vector discrete ordinate radiative transfer models for use in remote sensing retrieval problems. In *Light Scattering Reviews*, vol. 3, Kokhanovsky A. A. (ed.), New York: Springer 2008, pp. 229-278.

Spurr, R. and Christi, M, 2014: On the generation of atmospheric property Jacobians from the (V)LIDORT linearized radiative transfer models. *J. Quant. Spectrosc. Radiat. Transfer.* 142, 109-115.

Stam, D. M., De Haan, J. F., Hovenier, J. W., Stammes, P., 1999: Degree of linear polarization of light emerging from the cloudless atmosphere in the oxygen A band. *J Geophys Res,* 104, 16843-16858.

Tanré, D., F.M. Bréon, J.L. Deuzé, O. Dubovik, F. Ducos, P. François, P. Goloub, M. Herman, A. Lifermann, F. Waquet, 2011: Remote sensing of aerosols by using polarized, directional and spectral measurements within the A-Train: the PARASOL mission, *Atmos. Meas. Tech.*, 4, 1383-1395, doi:10.5194/amt-4-1383-1395.

Twomey, S., 1977: The influence of pollution on the shortwave albedo of clouds. *J. Atmos. Sci.*, 34, 1149–1152.

Van Diedenhoven, B., O.P. Hasekamp, and J. Landgraf, 2007: Retrieval of cloud parameters from satellite-based reflectance measurements in the ultraviolet and the oxygen A-band. *J. Geophys. Res.*, **112**, D15208, doi:10.1029/2006JD008155.

Vasilkov, A., Joiner, J.and Spurr, R., 2013: Note on rotational-Raman scattering in the O_2 A- and B-bands, *tmos. Meas. Tech.*, 6, 981-990, doi:10.5194/amt-6-981-2013.

Atmos. Meas. Tech. Discuss., doi:10.5194/amt-2015-340, 2016
Manuscript under review for journal Atmos. Meas. Tech.
Published: 18 January 2016

Vaughan, M., S. Young, D. Winker, K. Powell, A. Omar, Z. Liu, Y. Hu and C. Hostetler, 2004: Fully automated analysis of space-based lidar data: An overview of the CALIPSO retrieval algorithms and data products, *Proc. SPIE Int. Soc. Opt. Eng.*, 5575, 16–30.

Wang, J. Xu, X., Ding S., Zeng, J., Spurr, R., Liu X. et al., 2014: A numerical testbed for remote sensing of aerosols and its demonstration for evaluating retrieval synergy from a geostationary satellite constellation of geo-cape and goes-r. *J Quant Spectrosc Radiat Transf* http://dx.doi.org/10.1016/j.jqsrt.2014.03.020.

Wang, J., U. Nair and S.A. Christopher, 2004: GOES-8 Aerosol Optical thickness assimilation in a mesoscale model: Online integration of aerosol radiative effects. *J. Geophys. Res.,* 109, D23203, doi:10.1029/2004JD004827.

Wang, J., S. C. van den Heever and J. Reid, 2009: A conceptual model for the link between Central American biomass burning aerosols and severe weather over the south central United States, *Environ. Res. Lett.* 4, 015003, doi:10.1088/1748-9326/4/1/015003.

Winker, D., 2003: Accounting for multiple scattering in retrievals from space lidar, Proc. SPIE Int. Soc. Opt. Eng., 5059, 128–139.

Yamamoto, G., D. Q. Wark, 1961: Discussion of the Letter by R. A. Hanel, Determination of Cloud Altitude from a Satellite, *J. Geophy. Res.*, 66, 10, 3596.

Zarzycki, C. M. and Bond, T. C., 2010: How much can the vertical distribution of black carbon affect its global direct forcing? *Geophys. Res. Lett.,* 37, L20807.

Atmos. Meas. Tech. Discuss., doi:10.5194/amt-2015-340, 2016
Manuscript under review for journal Atmos. Meas. Tech.
Published: 18 January 2016

Atmospheric Measurement Techniques Discussions

Zeng, J., Q., Han, and J. Wang, 2008: High-spectral resolution simulation of polarization of skylight: Sensitivity to aerosol vertical profile, Geophys. Res. Lett., 35, L20801, doi:10.1029/2008GL035645.

Atmos. Meas. Tech. Discuss., doi:10.5194/amt-2015-340, 2016
Manuscript under review for journal Atmos. Meas. Tech.
Published: 18 January 2016

Atmospheric Measurement Techniques Discussions

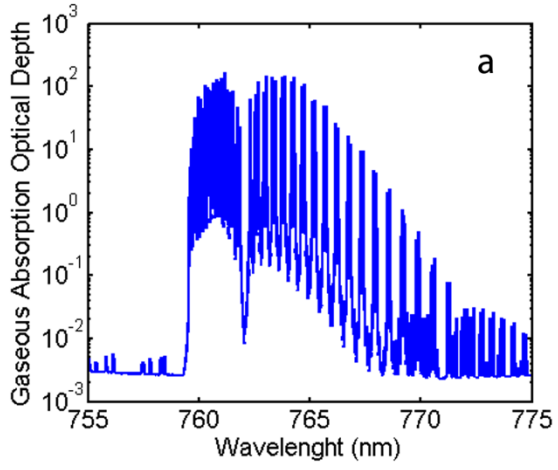

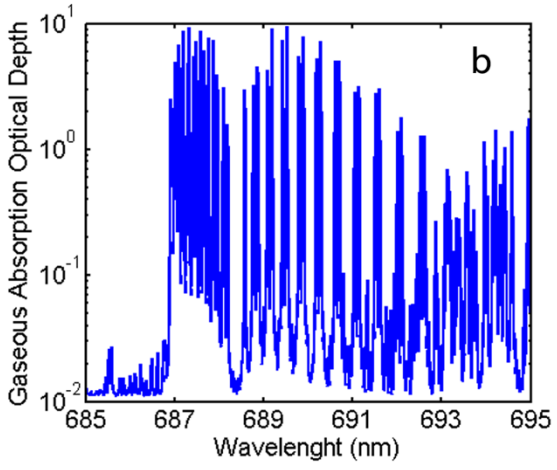

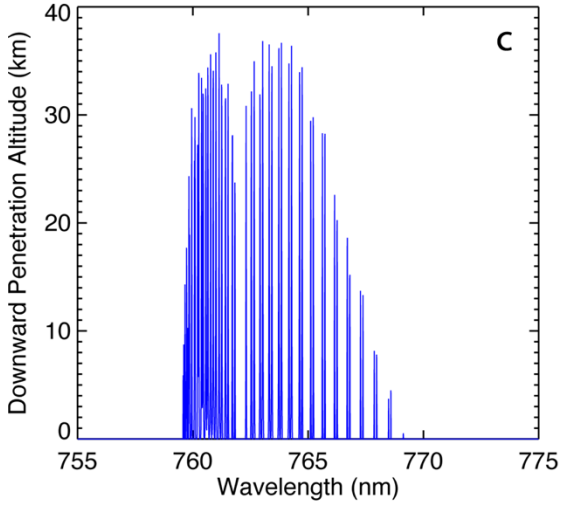

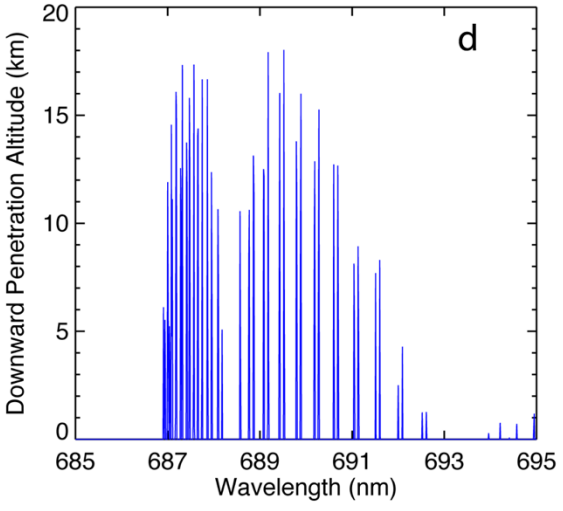

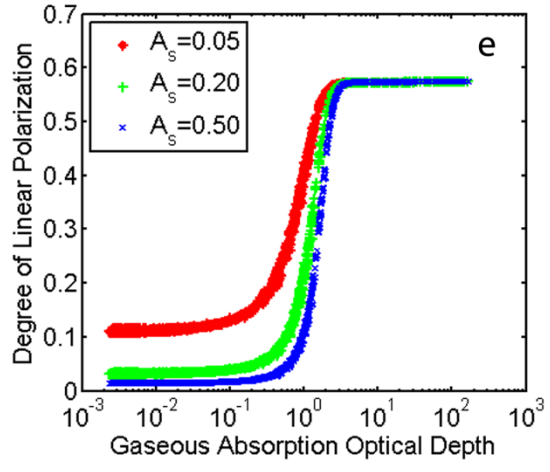

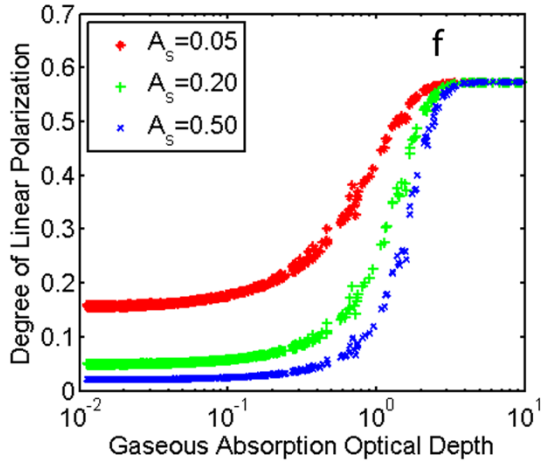

Atmos. Meas. Tech. Discuss., doi:10.5194/amt-2015-340, 2016
Manuscript under review for journal Atmos. Meas. Tech.
Published: 18 January 2016

Atmospheric Measurement Techniques Discussions

Figure 1. (a) Spectral absorption optical depth of atmosphere in the O_2 A band. (b) Same as in (a), but in O_2 B band. (c) penetration altitude for various wavelengths in the O_2 A band. (d) same as (c) but for the O_2 B band. The spectral interval and resolution (full-width at half maximum of a Gaussian spectral response) are 0.01 nm. The mid-latitude summer atmospheric profile is used in the calculation. (e) Degree of linear polarization as a function of gas absorption depth in the O_2 A band. (f) Same as in (e), but for the O_2 B band. The penetration altitude is defined as the altitude at which the intensity of the downward radiance is decreased by a factor of e as compared to its value at the top of the atmosphere. Note in atmospheric window channels the penetration altitude is set as zero (i.e., at the surface).

Atmos. Meas. Tech. Discuss., doi:10.5194/amt-2015-340, 2016
Manuscript under review for journal Atmos. Meas. Tech.
Published: 18 January 2016

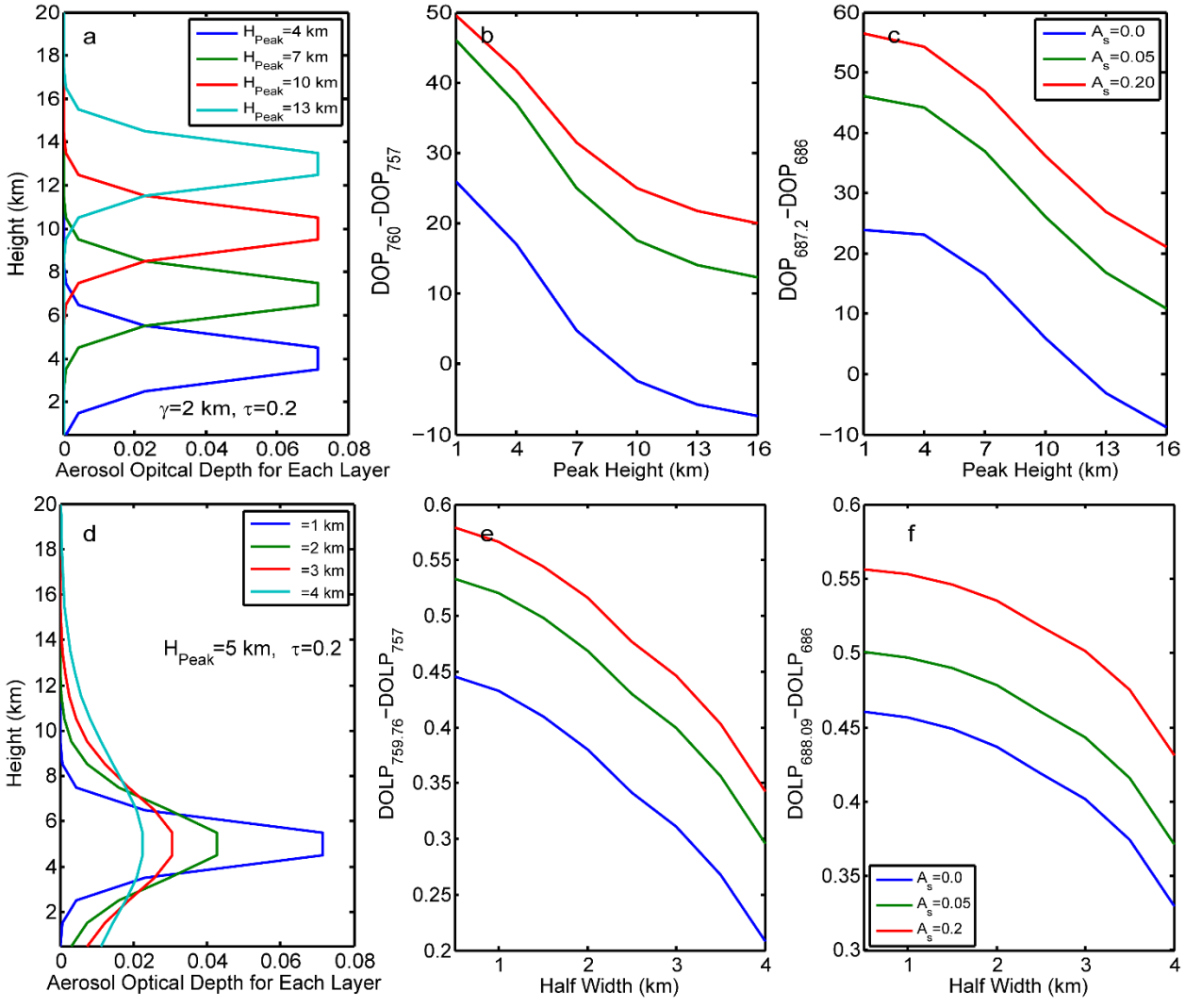

Figure 2: (a) The profile of aerosol optical depth for each layer; (b) Difference of DOLP between 759.98 (absorption channel in O_2 A band) and 757 nm (continuum channel) as a function the aerosol peak height for different surface albedos; (c) Same as (b) but for 687.2 (inside O_2 B band) and 686 nm (outside O_2 A band); (d) The profile of aerosol optical depth for different half width; (e–f) Same as (b–c) but as a function of half width at different absorption wavelengths (of 759.76 and 688.09 nm respectively). The solar zenith angle and view zenith angle are 66 ° and 0.0°, respectively.

Atmos. Meas. Tech. Discuss., doi:10.5194/amt-2015-340, 2016
Manuscript under review for journal Atmos. Meas. Tech.
Published: 18 January 2016

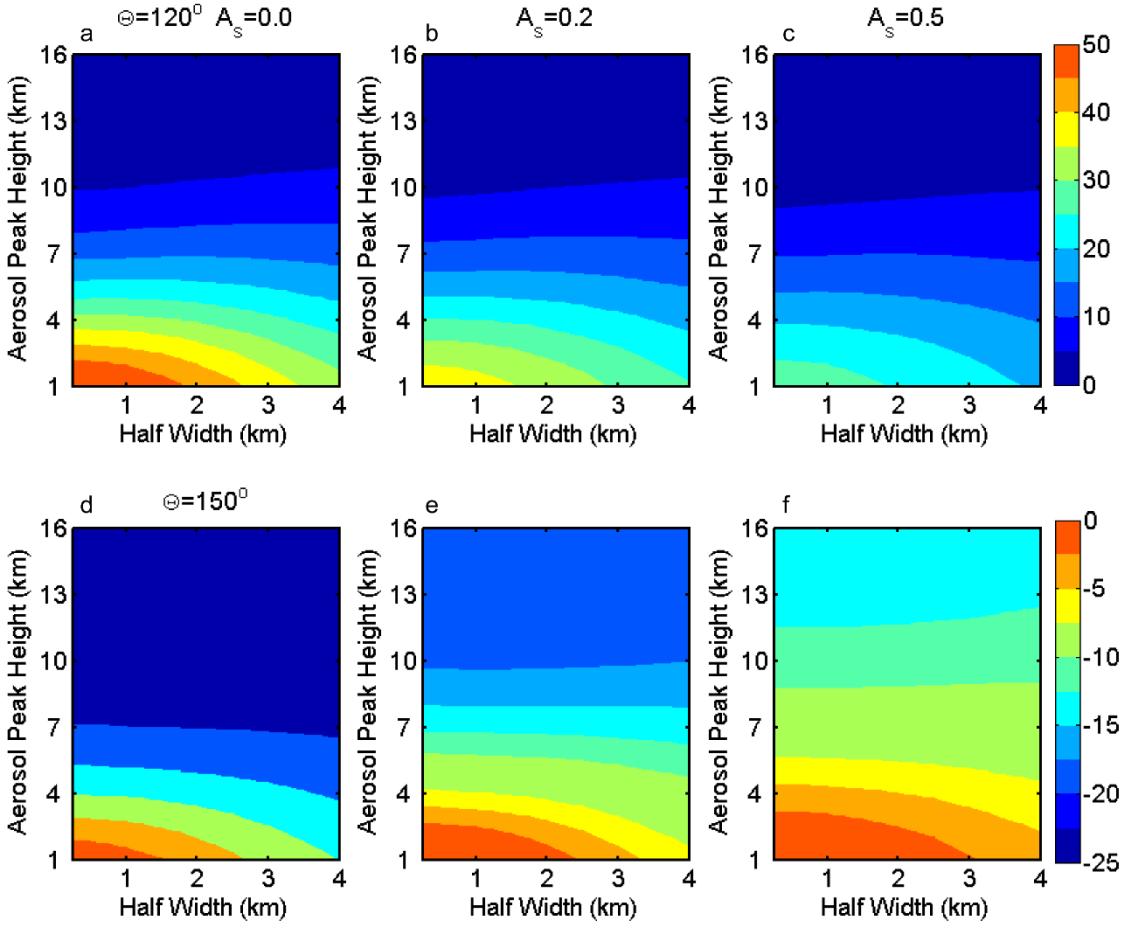

Figure 3. Contours of the DOLP at TOA as functions of aerosol peak height and half width at two different scattering angles, Θ =120° (upper panels) and Θ =150°(lower panels), for three different surface albedo, 0.0, 0.2 and 0.5. The wavelength is 759.98 nm.

Atmos. Meas. Tech. Discuss., doi:10.5194/amt-2015-340, 2016
Manuscript under review for journal Atmos. Meas. Tech.
Published: 18 January 2016

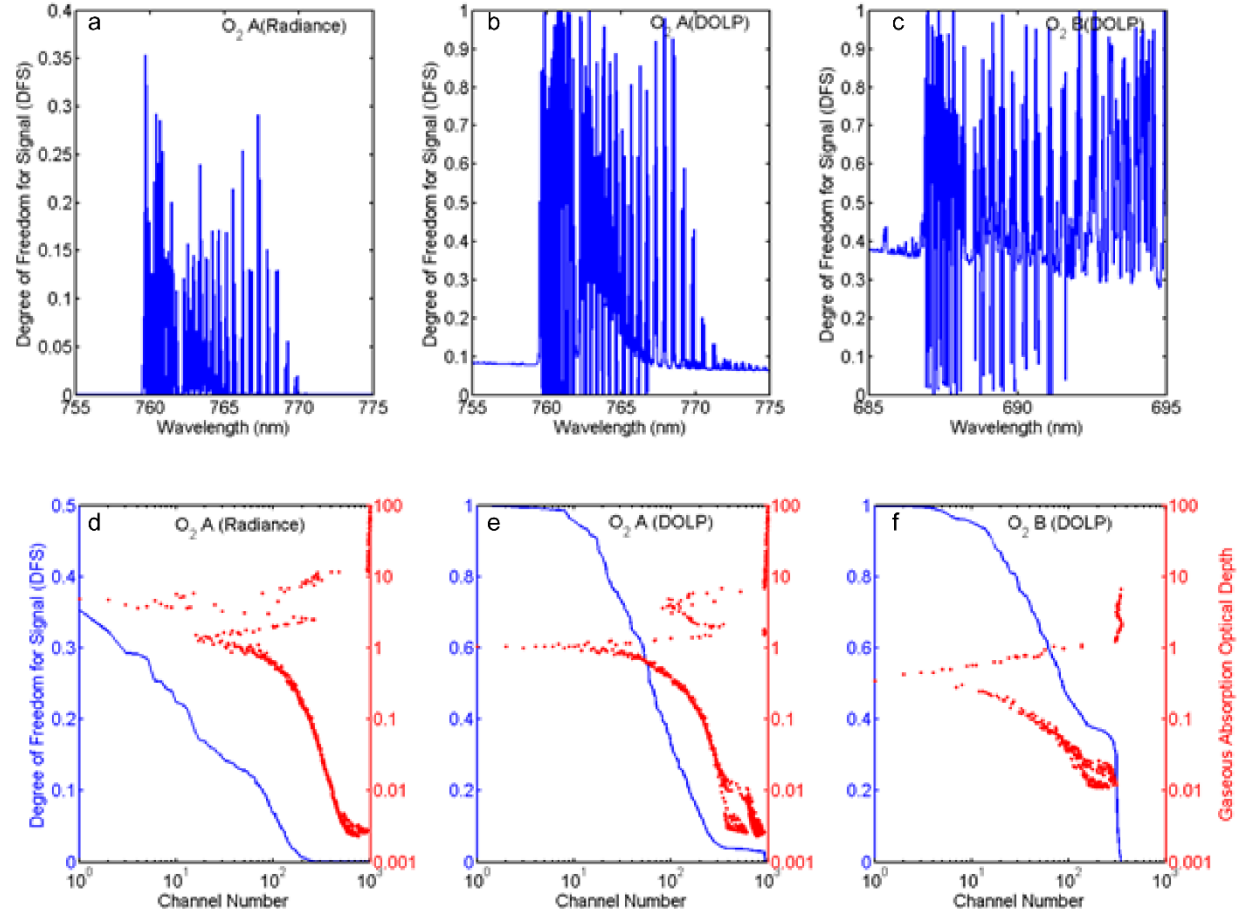

Figure 4. Degree of freedom for signal of individual channel within O_2 A and B bands, calculated from (a) radiance in O_2 A band, (b) DOLP in O_2 A band, and (c) DOLP in O_2 B band. (d) Sorted degree of freedom for signal (blue) calculated from radiance in O_2 A band, and corresponding gas absorption optical depth (red) for both O_2 A and B band. (e) and (f), same as (d), but calculated from DOLP in O_2 A and B bands, respectively.

Atmos. Meas. Tech. Discuss., doi:10.5194/amt-2015-340, 2016
Manuscript under review for journal Atmos. Meas. Tech.
Published: 18 January 2016

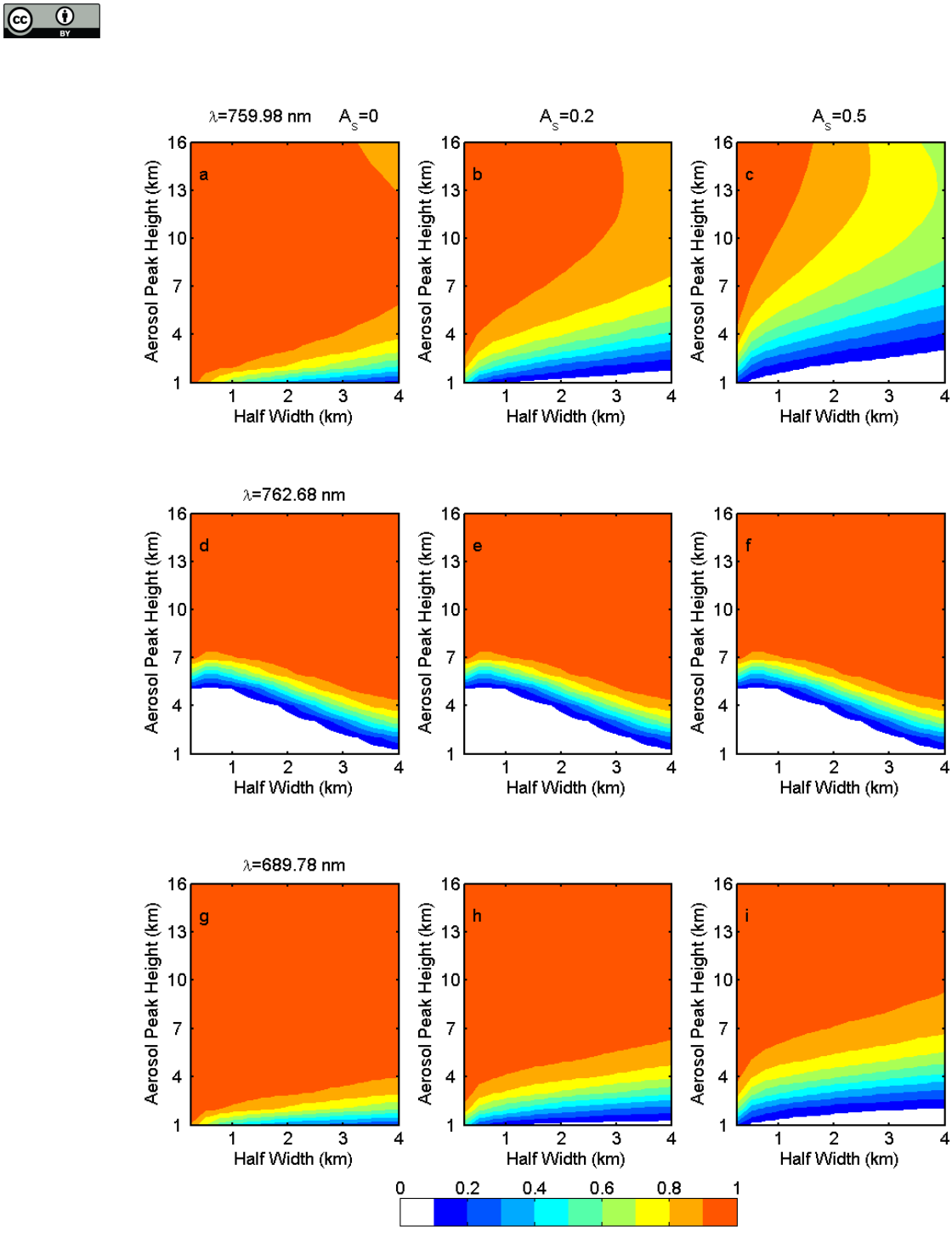

Figure 5. Contours of degree of freedom for signals of DOLP for retrieving aerosol peak height as a function of aerosol peak height H and half width at half maximum γ at three difference wavelengths in both O_2 A and B bands for different surface albedo, 0.0, 0.2 and 0.5. The gas absorption optical depths at wavelength 759.98, 762.68 and 689.78 nm, are 0.88, 2.73, and 0.34, respectively.

Atmos. Meas. Tech. Discuss., doi:10.5194/amt-2015-340, 2016
Manuscript under review for journal Atmos. Meas. Tech.
Published: 18 January 2016

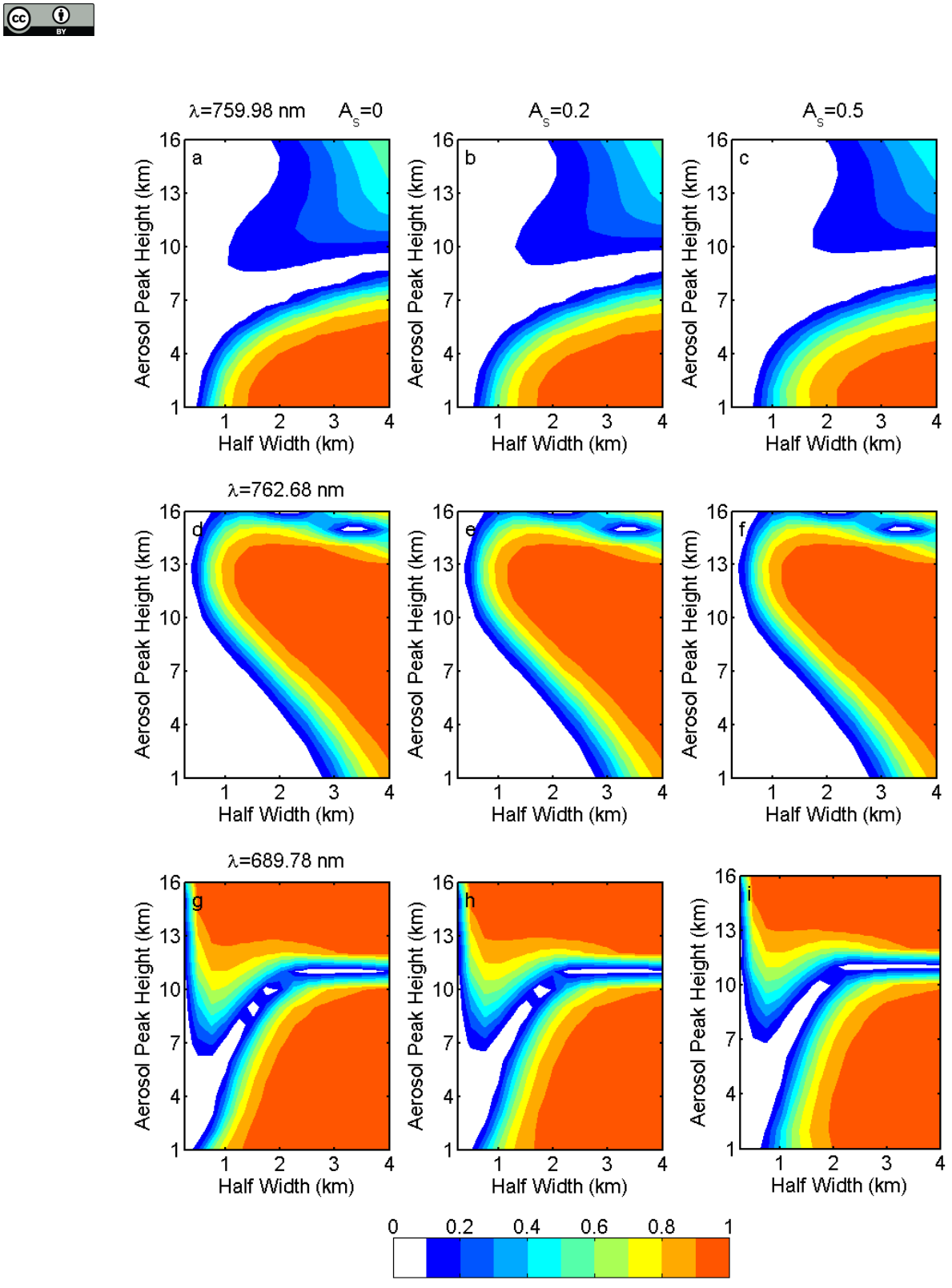

Figure 6 Same as Figure 5 but for the DFSs for retrieving profile half width.

Atmos. Meas. Tech. Discuss., doi:10.5194/amt-2015-340, 2016
Manuscript under review for journal Atmos. Meas. Tech.
Published: 18 January 2016

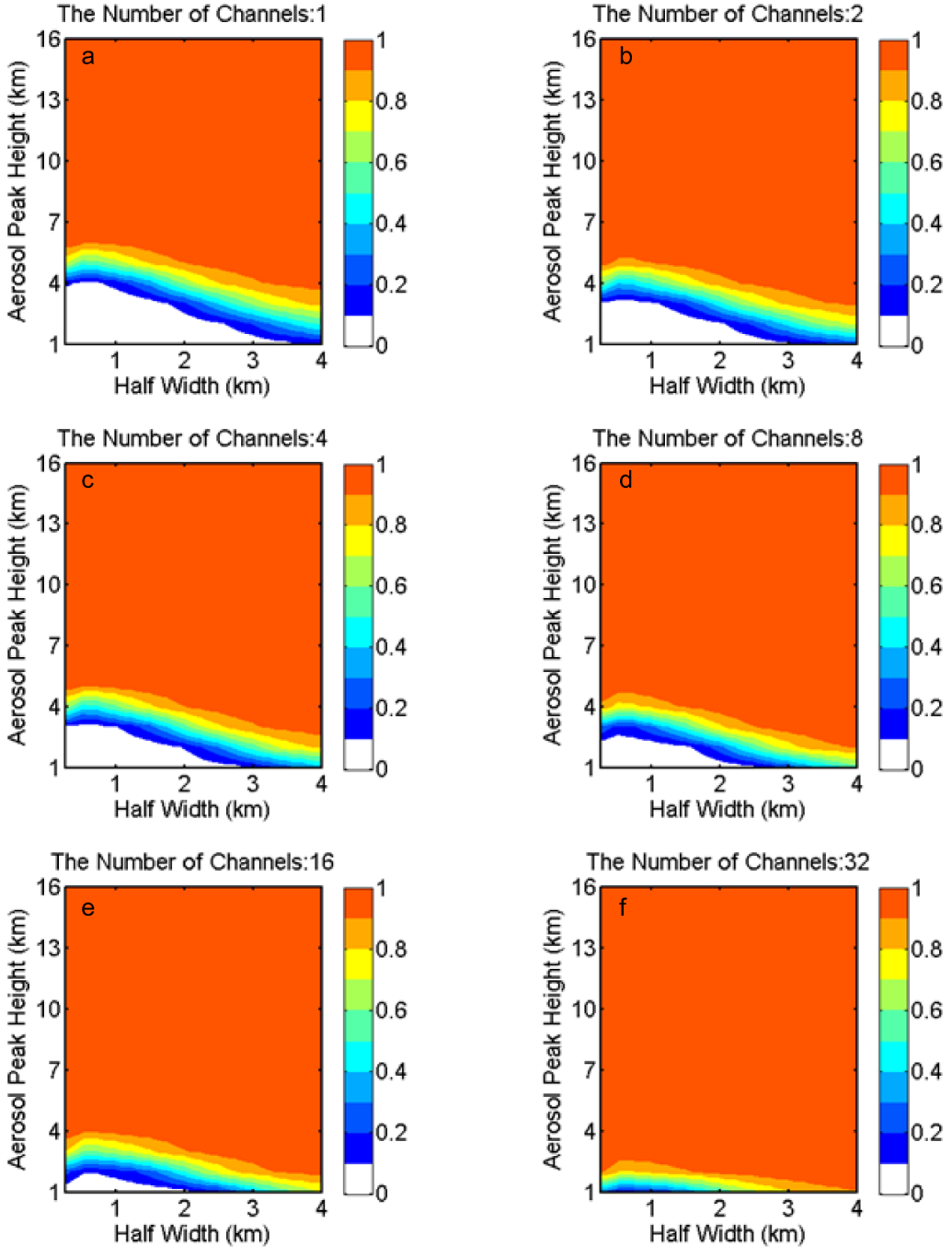

Figure 7. DFSs of DOLP for retrieving aerosol peak height calculated from various number (1, 2, 4, 8, 16 and 32) of selected channels in O_2 A band as a function of aerosol peak height and half width. The surface reflectance is assumed to be 0.2.

Atmos. Meas. Tech. Discuss., doi:10.5194/amt-2015-340, 2016
Manuscript under review for journal Atmos. Meas. Tech.
Published: 18 January 2016

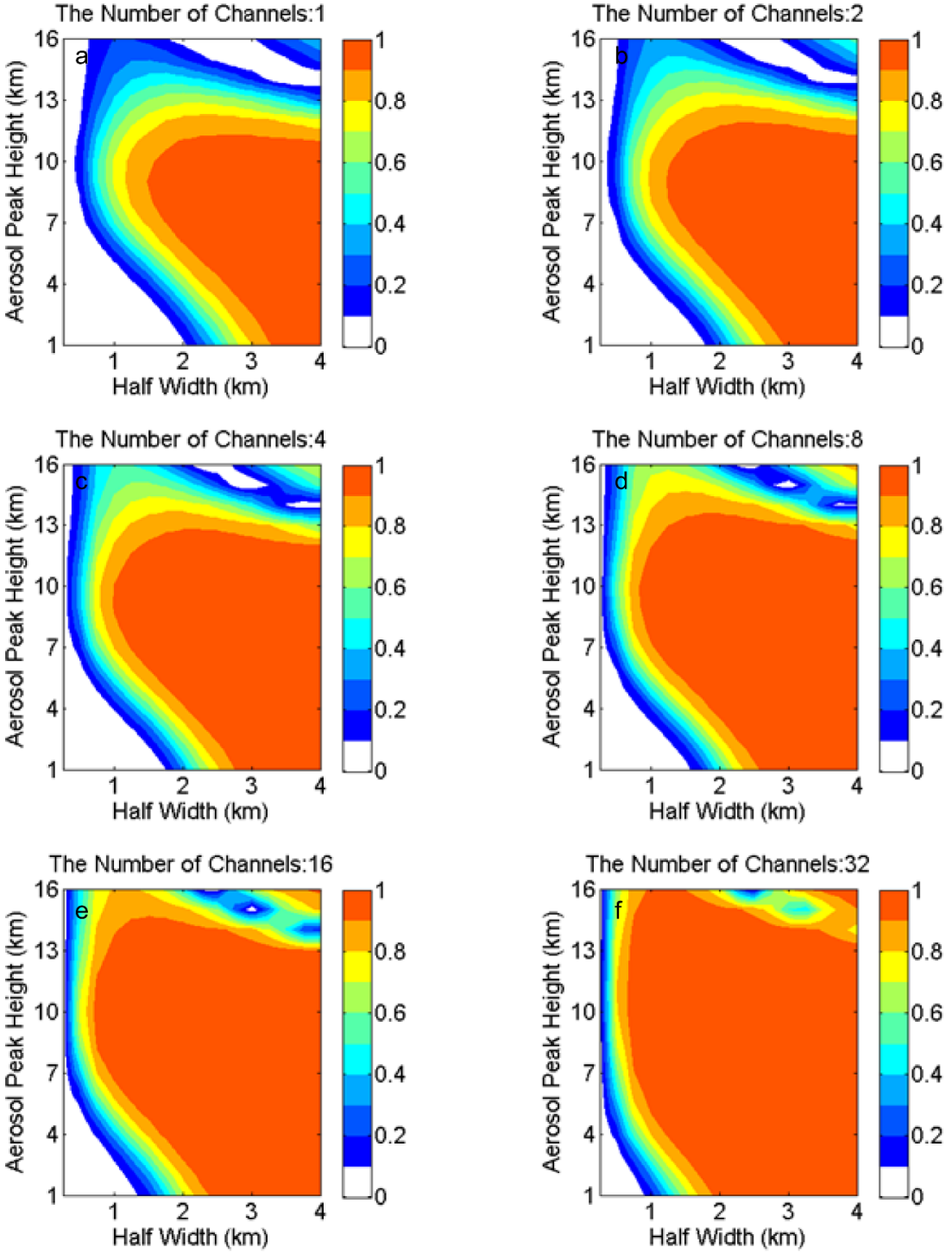

Figure 8. Same as Figure 7 but for DFSs for retrieving profile half-width.

Atmos. Meas. Tech. Discuss., doi:10.5194/amt-2015-340, 2016
Manuscript under review for journal Atmos. Meas. Tech.
Published: 18 January 2016

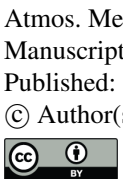

Atmospheric Measurement Techniques Discussions

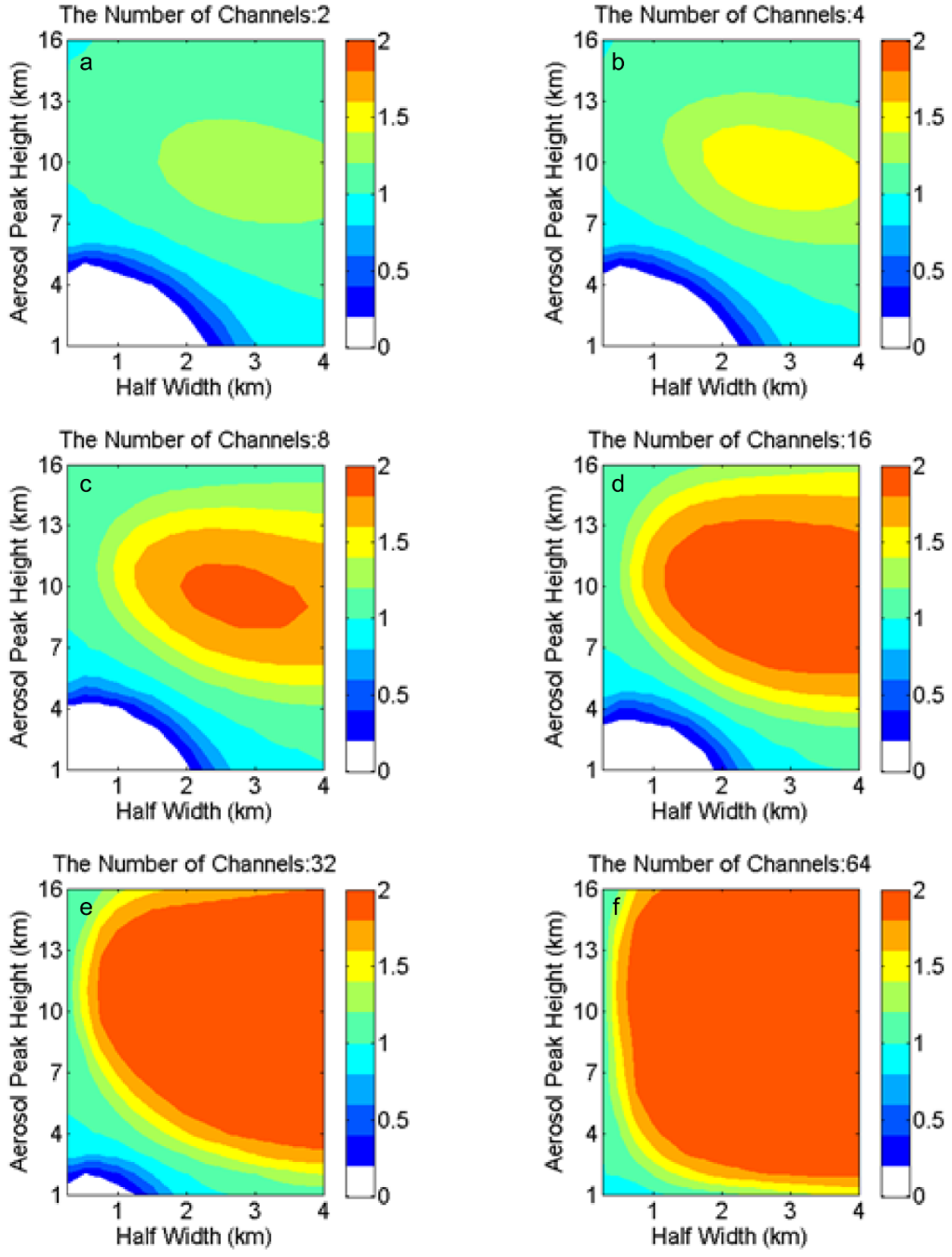

Figure 9. Contours of Degree of Freedom for Signals of DOLP for simultaneously retrieving aerosol profile peak height and half width calculated from various number (2, 4, 8, 16, 32and 64) of selected channels in O2 A band as a function of aerosol peak height and half width. The surface albedo is assumed to be 0.2.

Atmos. Meas. Tech. Discuss., doi:10.5194/amt-2015-340, 2016
Manuscript under review for journal Atmos. Meas. Tech.
Published: 18 January 2016

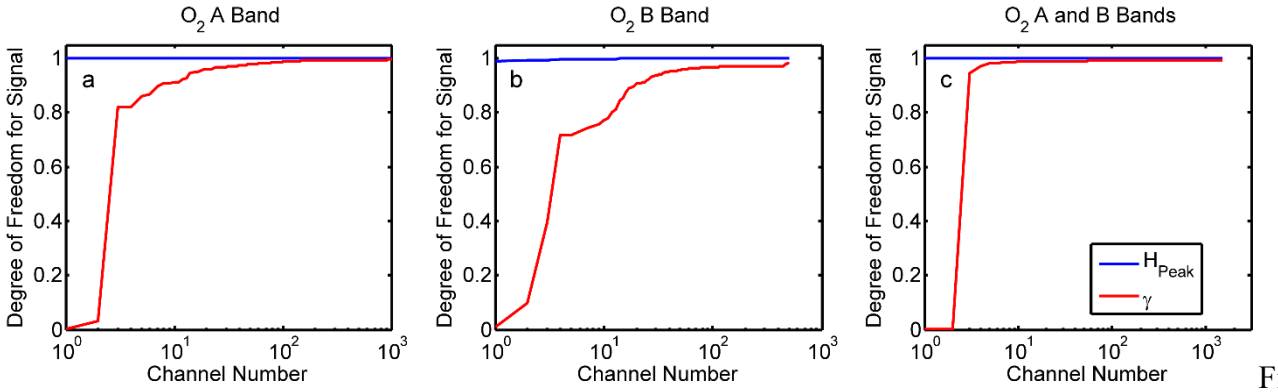

Figure 10. Degree of freedom for signal of DOLP for retrieving both aerosol peak height and half width as a function of the number selected channels from (a) O_2 A band, (b) O_2 B band, and (c) from O_2 A and B bands together.

Atmos. Meas. Tech. Discuss., doi:10.5194/amt-2015-340, 2016
Manuscript under review for journal Atmos. Meas. Tech.
Published: 18 January 2016

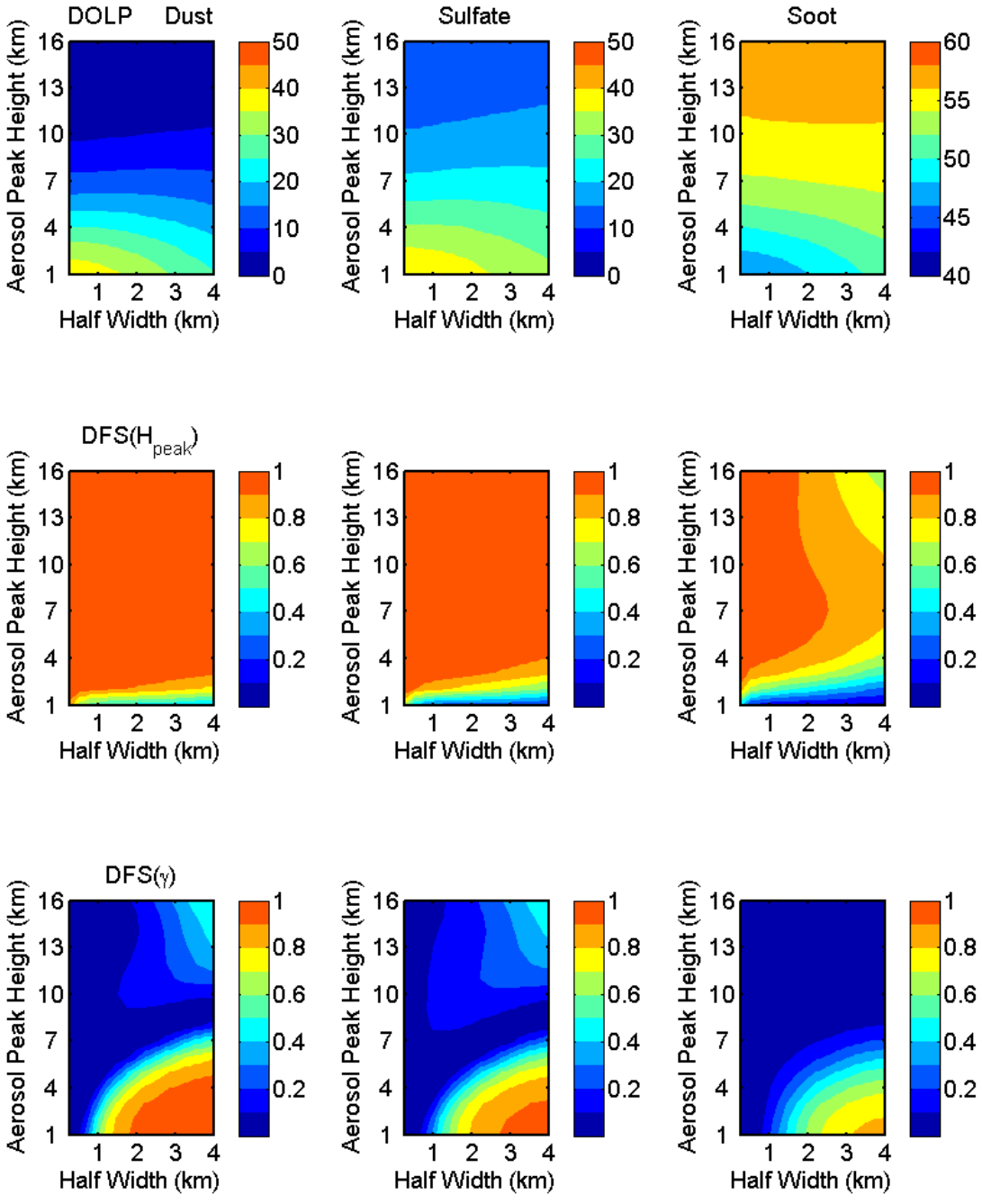

Figure 11. Contours of the DOLP at TOA and DFSs for three types of aerosols, dust, sulfate and soot, as functions of aerosol peak height and half width at the scattering angle 120°. The wavelength is 760 nm.

Atmos. Meas. Tech. Discuss., doi:10.5194/amt-2015-340, 2016
Manuscript under review for journal Atmos. Meas. Tech.
Published: 18 January 2016

Atmospheric Measurement Techniques Discussions

Table 1. The microphysical and optical properties of aerosols used in the simulations

Type	r_{eff} (μm)	v_{eff}	Refractive index
Dust	1.0	0.45	1.53-0.008*i*
Sulfate	0.5	0.45	1.428-2.05e-8*i*
soot	0.1	0.1	1.75-0.43*i*

70

Atmos. Meas. Tech. Discuss., doi:10.5194/amt-2015-340, 2016
Manuscript under review for journal Atmos. Meas. Tech.
Published: 18 January 2016

Atmospheric Measurement Techniques Discussions

Table 2. The first ten wavelengths selected for maximum contribution to the total information content from O_2 A and B bands.

No.	Wavelength (nm)	DFS*	
		H	γ
1	762.68	0.9998	0.0002
2	761.04	0.9998	0.0035
3	687.84	1.0000	0.9453
4	692.60	1.0000	0.9720
5	687.34	1.0000	0.9805
6	760.82	1.0000	0.9806
7	692.08	1.0000	0.9841
8	694.94	1.0000	0.9866
9	760.96	1.0000	0.9866
10	686.98	1.0000	0.9882

*DFS values for both peak height and half width corresponding to the channel number n are the result of information content analysis from a combined use of the first channel to channel number n.